

# POLITECNICO DI TORINO

**Master Degree in  
Biomedical Engineering**

## Multifunctional nanoparticles for dental applications



**Supervisor**

Prof. Chiara Tonda Turo

**Candidate**

Elena Montesarchio

**Co-Supervisors**

Prof. Gianluca Ciardelli  
Prof. Lino Ferreira  
Dr. Akhilesh Rai

Academic Year 2019/2020

# Index

Introduction.....	<b>5</b>
1. Tissue engineering .....	5
2. Dentistry (Endodontics).....	5
2.1 Tooth structure .....	5
2.2 Dental diseases.....	6
2.3 Endodontics and infections.....	7
3. MSCs.....	8
4. Bacterial infection .....	8
5. AMPs .....	9
5.1 Bacterial resistance .....	10
6. LL37-peptide.....	11
6.1 Role in odontogenic regeneration .....	14
7. Nanoparticles .....	15
7.1 NPs in dental applications .....	15
7.2 Gold NPs .....	17
7.3 LL37-AuNPs.....	19
8. Aim of the project .....	21
Materials and methods.....	<b>22</b>
1. Materials .....	22
2. Nanoparticles preparation .....	24
3. Bacterial culture .....	26
3.1 Green laser .....	27
3.2 Antimicrobial test .....	28
3.3 Bactericidal mechanism: permeabilization .....	30
4. Cell culture.....	31
4.1 Cell viability .....	32
4.2 Cell proliferation.....	34
4.3 Mechanism of interaction: EGF receptor.....	36
4.4 Cell differentiation .....	39
4.4.1 ALP test.....	40
4.4.2 Alizarin-Red Staining.....	41

<b>Results</b> .....	<b>44</b>
1. Antimicrobial test .....	44
2. Permeabilization .....	46
3. Cell viability .....	47
4. Cell proliferation .....	48
5. EGFR expression .....	49
6. Cell differentiation .....	51
6.1 Single administration.....	51
6.2 Multiple dosing.....	53
6.3 Limited-time single administration with poor culture medium.....	54
<b>Scaffold in regenerative endodontics</b> .....	<b>57</b>
1. Gelatin-LL37-AuNPs nanofibrous scaffold.....	57
2. Nanofibres preparation.....	60
3. Conjugation.....	61
4. Antimicrobial test .....	63
<b>Conclusions</b> .....	<b>67</b>
<b>References</b> .....	<b>70</b>

## Index of figures

Figure 1- Human dental structure [3] .....	5
Figure 2-SCAPs three days after seeding [11] .....	8
Figure 3- Mechanisms of interaction between AMPs and the host membrane [15]. .....	10
Figure 4-hCAP18 [65]. .....	12
Figure 5-Helical secondary structure of LL37-peptide [14]. .....	12
Figure 6-different experimental conditions of synthesis of Au NP in the presence of a peptide (CM) [46]. .....	20
Figure 7-BD Accuri C6 benchtop flow cytometer [68] .....	23
Figure 8-Procedure scheme for green laser exposition .....	28
Figure 9-The luciferase reaction [66] .....	33
Figure 10-IN CELL image of SCAPs after 48h from the treatment (only cells). The blue channel (Hoechst) are lived cells, the red channel (PI ) are apoptotic or dead cells. ....	35
Figure 11-Schematic diagram of a flow cytometer [67] .....	38
Figure 12-Antimicrobial test of LL37-Au NPs (60 µg/mL) and Au NPs (60 µg/mL) in 10% human serum. ....	45
Figura 13-Permeabilization of the <i>E. coli ML-35p</i> membrane using NPs and laser. On the left the results for the external membrane (OM) on the right those for the internal membrane (IM). .....	46
Figure 14-On the left calibration curve of <i>CellTiter-Glo® Luminescent Cell Viability Assay</i> with SCAPs. On the right, cell viability test results. ....	47
Figure 15-Percentage histogram for the cell proliferation test. ....	48
Figure 16-Graph showing the fluorescence of control cells and cells labelled with Alexa Fluor 488, used to choose the fluorescence threshold. ....	49
Figure 17-LL37-AuNPs treated cells compared with untreated cells (left) and free peptide treated cells (right). ....	50
Figure 18-Mean Fluorescence Intensity histogram. ....	50
Figure 19-Microscopic images showing the folding of the cell monolayer. They refer to culture in differentiation medium after 10, 12 and 13 days respectively from left to right. The elongated shape of the migrating cells can be seen. ....	51

Figure 20-ALP test performed after 7 days of culture with single administration. ....	52
Figure 21-Alizarin Red Staining performed after 18 days of culture with single administration and an experimental setting scheme (on the right the samples grown with a differentiation medium). The images were acquired with a scanner. ....	52
Figure 22-ALP test performed after 7 days of culture with multiple administration.....	53
Figure 23-Alizarin Red Staining performed after 16 days of culture with multiple administration and an experimental setting scheme (on the right the samples grown with a differentiation medium). The images were acquired with a scanner. ....	54
Figure 24-ALP test performed after 7 days of culture with 4h single administration in 1% V/V Pen/Strep in KO-DMEM.....	55
Figure 25- Cells 48h cells after treatment with poor culture medium.....	55
Figure 26- Cells 48h cells after treatment with poor culture medium and AuNPs (60µg/ml).....	55
Figure 27- Cells 48h cells after treatment with poor culture medium and LL37-AuNPs (60µg/ml).....	55
Figure 28- Alizarin Red Staining performed after 18 days of culture with 4h single administration in 1% V/V Pen/Strep in KO-DMEM and an experimental setting scheme (on the right the samples grown with a differentiation medium). The images were acquired with a camera.....	56
Figure 29-Diagram of the electrospinning process [58].....	58
Figure 30- The equation represents the reaction between oxirane rings on the GPTMS and amino groups on the gelatin chains and the acid catalyzed hydrolysis that generates the pendant silanol groups (Si-OH). [59] .....	60
Figure 31-The equation represents the condensation between two silane groups, Si-O-Si bond is formed [59].....	60
Figure 32-Different approaches to create composite fibrous materials engineered by electrospinning [58].....	62
Figure 33-Procedure scheme for green laser exposition with fibers .....	64
Figure 34- Antimicrobial test of LL37-Au NPs-Fibers and Au NPs Fibers in 10% human serum. ....	65
Figure 35-Permeabilization of the <i>E. coli</i> ML-35p membrane. On the left the results for the external membrane (OM) on the right those for the internal membrane (IM). ....	66

## Introduction

### 1. Tissue engineering

Tissue engineering comes from the union of knowledge in the chemical, biological and materialistic fields. This knowledge is used to regenerate, repair or modify a biological tissue, in other words to engineer such tissue for specific applications. From the field of materials, notions are drawn regarding the structure of the scaffolds, the synthesis methods and the chemical-physical properties that determine its applications, factors affecting the mechanical response and degradation of the structure in relation to changes in pH, the presence of water, proteins, ions and so on. The biological environment is very complex and aggressive for many materials, for example corrosion of the metals. Thus, tissue engineering is used to evolve the structure of nanomaterials in a desired direction.. When trying to model a biological system like a tissue one must perceive every aspect, every small molecule as well as a residual stress in the material that could interfere the biological pathways. The high costs and the difficulty in predicting any problems make tissue engineering still a little used in medical applications [1].

### 2. Dentistry (Endodontics)

One of the most beaten roads is of the dental one. The frequency with which an average individual is faced with a dental problem is much higher than any other health problem.

#### 2.1 Tooth structure

The teeth are rigid structures, which are used for chewing and biting of foods. Teeth are present in the mouth of many animals. Teeth are composed of multiple tissues with a different density and function. In human, they protrude from the gum and are pervaded by vessels and nerves. Starting from the outside, a tooth has enamel that covers the crown, the part of the tooth that

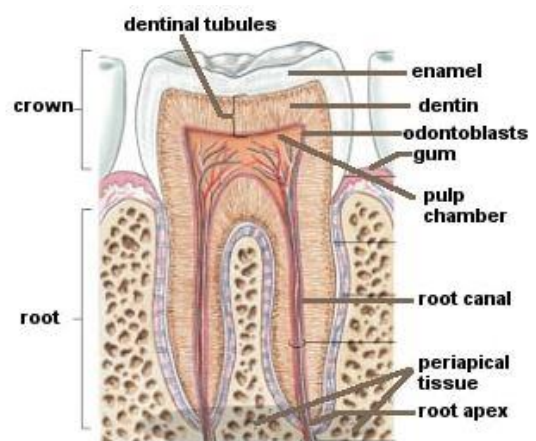


Figure 1- Human dental structure [3]

emerges from the gum, and the cementum that covers the root. The enamel is a very hard tissue, with high percentage of mineralization (96%), while the cementum is softer

and has the important task of acting as an intermediary between the tooth and the periodontal ligaments of the jaw. Additionally, inside the tooth, there is a dentin, which is a thick but less dense bone layer than the enamel, it is the real volumetric mass of the tooth. The enamel is a hard but also fragile substance which, without the elasticity of the underlying dentine that acts as a support, would not resist to heavy loads. Tooth has tubular structures, dental canaliculi, which are used to supply the entire tooth with blood and become thinner when move away from the pulp. These structures greatly increase the degree of permeability of the dentine making it more easily perishable from an infection and susceptible to pain. Primary odontoblasts, during tooth development, form the primary dentine and, after the eruption, generate the secondary dentin. Tertiary dentine is formed only if traumas occur or harmful stimuli are felt, for example bacterial toxins. It is part of the repair process; where the dentine undergoes damage, the tertiary dentin is created. The tertiary dentine is divided into reactionary dentin, borne by the surviving post-mitotic primary odontoblasts, and restorative dentine, generated by odontogenic stem / progenitor cells that ,recruited, differentiate into new odontoblasts [2]. During dentinogenesis, odontoblasts release the extracellular matrix by retreating to create a dense layer of cells between dentine and predentine, this layer delimits the pulp chamber. The pulp is the heart of the tooth, containing blood vessels and the nerve that germinate from the mandibular bone and through the papilla [3]. Depending on the type of tooth, there can be multiple roots, which determines the external shape.

## 2.2 Dental diseases

There are following most common diseases borne by teeth and gums:

- tooth decay, certainly the most common also called 'caries', which is a progressive deterioration of the tooth and its structures caused by the combination of the presence of bacterial population with sugar (bacteria produce acids that degrade hard tissues) [4]
- periodontal disease, which is an inflammation of the gum characterized by redness, swelling and bleeding; it is also caused by bacterial infection [5]
- dental plaque or oral biofilm is a dense layer of bacteria that can quickly lead to the cavity [6]

- dental abscess, which is an advanced state of immune response to infection, leads to accumulation of pus (white blood cells that fail to eradicate the infection and thus accumulate more and more on the site) [7].

Therefore, trauma and systemic diseases that not only concern the teeth but also the bone or neuronal tissue. Bacterial infections are the main cause of dental disorders. These infections, although very common, should not be underestimated because if they are not resolved in time, they can become systemic.

### 2.3 Endodontics and infections

If the bacteria enter the bloodstream (Bacteremia), lead to pathologies such as infections of the main organs or sepsis. The most vulnerable subjects are those who have undergone a prosthesis and those who have congenital heart defects or immunocompromisation. The treatments generally involve a restoration of the morphology of the tooth to avoid further problems, and is considered as the dental restoration [8]. Mouldable materials are used to reconstruct the parts of the tooth that have deteriorated or have been removed for the dental surgery. It is essential, in fact, to allow the patient to chew, regain the aesthetics of the smile and, last but not least, to occlude a cavity that could accumulate food residues and be an excellent place for the growth of bacterial colonies. If the infection is deeper it is necessary to intervene on the root of the tooth, the dental surgery is more invasive and complex as root canals and pulp chamber are inhabited by blood vessels. The endodontic therapy involves the removal of these tissues, the decontamination of cavities and the sealing. Irrigators are used for decontamination, the most common being used are Sodium hypochlorite (NaClO) (between 0.5% and 5.25%) and 2% chlorhexidine gluconate. They are toxic and therefore the tooth is surrounded by rubber barriers. At the end of the procedure a natural polymer, gutta-percha, is used as a sealant. Odontoblasts intervene to protect the papilla from exogenous material. Therefore, it is important to study the cytotoxicity of the materials used for dental repairs. Odontoblasts, highly specialized postmitotic cells, are difficult to cultivate for in vitro tests. For this purpose, differentiated stem cells, the so-called odontoblast-like cells (OLC), are often used [9]. Anyway, the tooth has only a mechanical function. Furthermore, it is advisable to follow a conservative approach in order to reach a treatment capable of two main processes. These processes include a regeneration treatment and a protective one. The aim is to obtain a healthy tooth without any kind of foreign material. One technique is regenerative endodontic



procedures (REPs), which is based on stem cells but generates a cement-like substance or cementum-like tissue. Clinical success is high when defined as apical healing periodontitis and possibly restoration of nerve function. However we consider the clinical success from the histological point of view, described as regeneration of complex pulp-dentin cells and regeneration of tissues such as nerves, blood vessels and dentin, the results are positive only in the absence of bacteria [10]. In the current protocol, a disinfectant irrigant (NaOCl 1.5%) is used which is not sufficient to remove bacteria due to the shape of the root canals. NaOCl can not be used in REP technique due to cytotoxicity of NaOCl to stem cells. Another example such as nitric oxide synthases (NO donors), is able to differentiate DPSCs and stimulate the formation of tertiary dentin, a clonogenic population with stem cell-like properties into odontoblast-like cells [2]

### 3. MSCs

The knowledge of the dentin-pulp complex pushes the research of recent years towards new therapies based on self-regeneration of the tooth. There are many approaches suggested by tissue engineering and one of the most promising routes is application of progenitor / stem cells. Stem cells are cells in the undifferentiated state characterized by a certain potency and self-renewal capacity; therefore, they can differentiate into series of cell lineages and despite the innumerable cell divisions they do not lose this property. Stem cells of apical papilla (SCAPs), from the most apical part of the root, have the potential to differentiate into osteogenic, adipogenic, myogenic, and chondrogenic cells. There are different types of stem cells in the tooth, the most studied are the dental pulp stem cells (DPSCs) but SCAPs show a higher proliferation and mineralization potential [11]. The basic idea therefore is to use this multipotency to induce the regeneration of damaged tissue. The major causes of dental damage are traumas or infections that in the

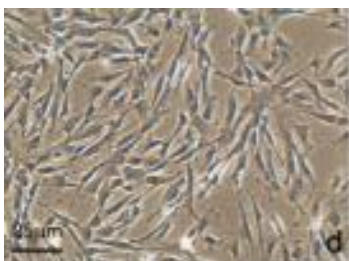


Figure 2-SCAPs three days after seeding [11]

worst cases can lead to complete tissue necrosis. In this project a novel nanoformulation containing antimicrobial peptide was developed that would allow odontological regeneration while limiting the major cause of damage, namely bacterial infection. For this purpose, an antimicrobial peptide (LL37) was selected which is able to differentiate mesenchymal stem cells of the dental pulp into odontoblasts.

#### **4. Bacterial infections**

Bacteria have inhabited the Earth for a long time and have adapted to almost all environmental conditions [12]. Bacteria make up the most important biomass on our planet. In humans they are naturally present mainly in the intestine, make up the bacterial flora, and on the skin. Despite this codependency, many bacteria are pathogenic and can lead to serious, even fatal, infections.

Compared to eukaryotic cells, bacteria are about ten times smaller and have different shapes, given by the cell wall and cytoskeleton, which allow them to move. They live in colonies, some species gather in particular superstructures, for example, creating filaments. When they stabilize in an environment they create the so-called biofilm to protect from the adverse condition. A biofilm is composed of countless bacteria protected by a polymeric matrix composed of polysaccharides, DNA and proteins produced by the bacteria themselves. Bacterial biofilms are much more difficult to treat as they resist both antibiotics and disinfectant chemicals.

In biofilm, the metabolism of bacteria is slowed down and this makes them more resistant. There is a gradient of nutrients from the biofilm surface to the bottom where anaerobic 'dormant' cells reside. Biofilm inhibits the activity of drugs and therefore higher MIC is needed to kill bacteria. In fact, bacteria use biological signaling, the so-called quorum sensing (QS), and are able to understand cell density and generate fruiting bodies from which the endospores detach (inactive and highly resistant bacteria versions) to infect other places. Biofilm could be present on natural surfaces such as teeth but also in various other organs and they become chronic pathology. Preventing an infection that has already reached the stage of biofilm formation is really complex,. [13].

Bacteria are classified into Gram-positive and Gram-negative. They essentially differ in the composition of the cell wall, the Gram-positive bacteria have a lipid (internal) membrane and a thick layer of peptidoglycan while Gram-negative bacteria have thinner cell wall but the lipid membranes have two layers (both external and internal). The infection begins with colonization, when the microorganism enters the body and multiplies. Infection does not occur easily in healthy individuals, as there are many defense barriers, however who have a compromised immune system or simply an open wound, it is much simpler to get an infection. Orifices such as the oral cavity are excellent access doors to get bacterial infection.

#### **5. Antimicrobial peptides (AMPs)**

Several AMPs (antimicrobial peptides) are known in the literature. AMPs are part of the innate immune response, they are powerful broad-spectrum antibiotics that have been found in many living beings. One of their peculiarities is the ability to fit inside a cell membrane as they are amphiphilic, meaning they have hydrophobic and hydrophilic residues. Amphiphilicity allows them to create pores in bacteria and thus destabilizing the bacterial cell membrane, leading to bacterial death [14].

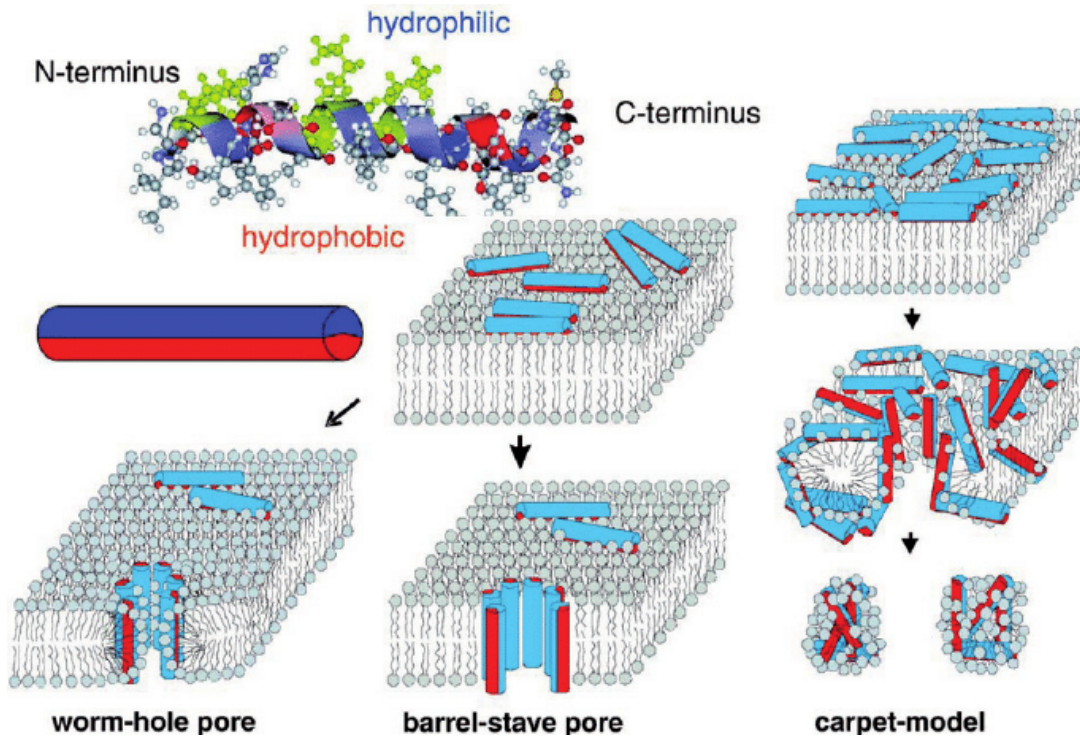


Figure 3- Mechanisms of interaction between AMPs and the host membrane [15].

AMPs not only use permeabilization mechanism to kill bacteria but also affect the synthesis of DNA or proteins. The first contact takes place by electrostatic interaction, in fact the bacterial cells are mostly anionic and the antimicrobial peptides are slightly positively charged followed by penetration of AMPs into membrane. In recent studies, bactericidal properties of AMPs have been reported. Importantly, there is poor interaction between AMPs and mammalian cell membrane due to their transmembrane potential. Bacterial membranes are in fact rich in acid phospholipids. The contact between peptide and cells is much rarer than that between bacteria and peptide, which makes this mechanism selective and the AMPs less cytotoxic. The cholesterol in the host cells serves to stabilize the membrane and in addition, by interacting with the peptide, it limits its possible action. Over the years, specific peptides have been engineered to understand the mechanisms of interaction between AMPs and cell membranes.

## 5.1 Bacterial resistance

The main problem in the fight against infections is that bacteria develop antibiotic resistance. It is increasingly a global issue that would require legislation to control the usage of antibiotics. Antibiotics increase selective pressure while killing the weakest bacteria and push the new generation mutate. These bacteria have horizontal gene transfer (HGT) of resistance genes called antibiotic resistance genes (ARGs) [16]. An emphasis should be placed on infections in healthcare facilities; for example, the hospital is one of the outbreaks of methicillin-resistant *Staphylococcus aureus* (MRSA) in which medical personnel are exposed and can therefore act as a vehicle among patients if the necessary hygiene precautions are not taken [17]. The genetic mutation process can occur in bacteria in years of evolution, but bacteria can develop resistance against antibiotics rapidly [18]. There are alternative therapies, one of them is based on the use of exogenous AMPs. The bacteria can also develop mutations to resist the attack of AMP, for example by modifying the surface charge, adopting different membrane mutations or secreting proteases in order to degrade the AMPs.

## 6. LL37-peptide

Discovered in 1995, LL37 is an AMP and in particular it is part of the Cathelicidin family. LL37 peptides have antimicrobial, skin regeneration, blood vessel formation and immunomodulatory properties. Cathelicidin are the first actors of innate immunity in mammals. They are called Cathelicidin because they present a highly conserved cathelin domain, the first time it was discovered in pig leukocytes and classified as inhibitor for the cysteine proteinase cathepsin L (then it turned out it was not true, but the name remained). In mammals, several antimicrobial peptides of cathelicidine family have been identified but in humans only one of 18kDa has been found, hence called hCAMP18. [14]The whole hCAMP18 protein complex can be schematized in three parts: there is a central body characteristic of cathelicidines composed of about 100 residues, at the N-terminus there is a signal peptide formed by about 30 residues which is eliminated as soon as it accomplishes its purpose, namely the exocytosis or storage of the protein complex, finally there is the antimicrobial peptide with the C-terminus.

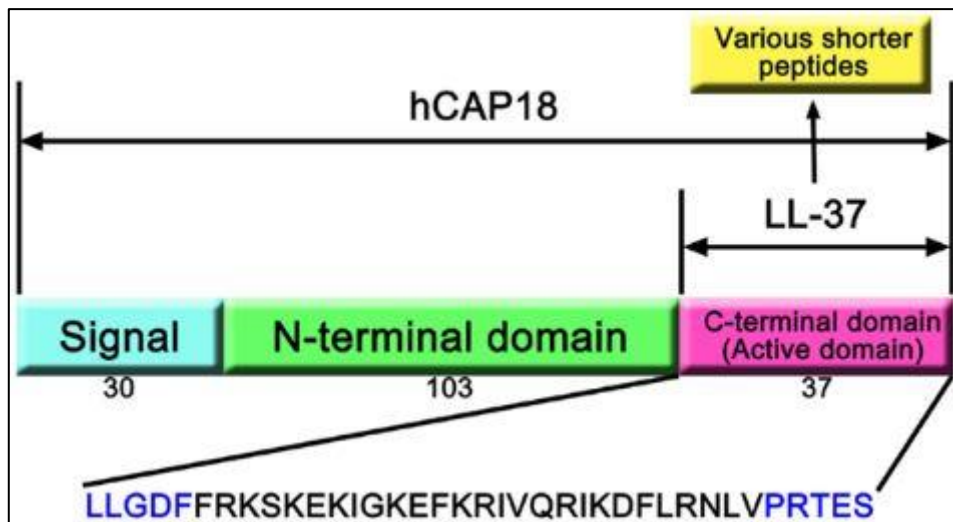


Figure 4-hCAP18 [65].

Once the AMP is freed from the portion of catelicidine, LL37 is released by proteinase 3-mediated extracellular cleavage (at Ala-Leu site). LL37 has been found in many areas of the human body such as the skin, the respiratory tract and the gastrointestinal tract, and as well as in immune cells.

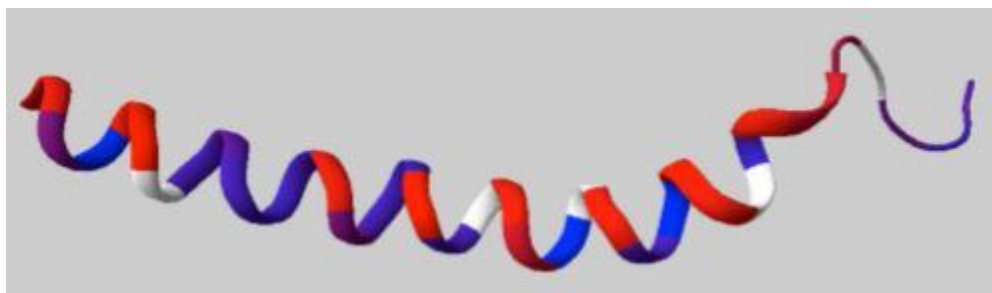


Figure 5-Helical secondary structure of LL37-peptide [14].

LL37 peptides have 37 amino acids starting from the two Leucins (LLGDFFRKSKEKIGKEFKRIVQRIKDFLRNLPRTES). The amino acid sequence indicates the amphiphilic nature of the peptide, 54% of the residues are hydrophilic (6 Lys and 5 Arg residues are positively charged at physiological pH and 3 Glu and 2 Asp residues are negatively charged) which provide a positive charge of +6 [19]. The secondary  $\alpha$ -helix structure arranges the hydrophobic residues on one side and the hydrophilic ones on the otherside to protect its amphipathic nature. Three-dimensional NMR showed that the helical region is from 2 to 30, while the C-terminus is mobile [14]. Unlike many helical AMPs, LL37 occurs in this form not only when it is associated with a membrane but

already in an aqueous saline environment. This tendency to create a superstructure makes the peptide more 'rigid'. Nanoformulation could help in this regard. LL37 is proposed as a periodontal therapeutic agent as saliva is hypotonic and this type of environment improves the antimicrobial performance of the peptide. But saliva is also rich in carbonate which induces oligomerization. The peptide in itself is very sensitive to environmental factors, such as proteases therefore a stable nanoformulation is needed [20], [21]. The bactericidal mechanism initially proposed was the so-called 'carpet mechanism' (the peptide accumulates superficially to the membrane up to the breaking point, critical lytic concentration), now, instead, the researchers are more likely to endorse the hypothesis of a 'toroidal pore mechanism' (showing the hydrophobic part of the tails of the double phospholipidic layer of bacterial membranes) which would also be helped by oligomerization. The damage is not permanent, the toroidal pores collapse almost instantaneously, but it is enough to create a leakage of cytoplasmic material or a perturbation of the bacterium's membrane which, if it does not kill it, still blocks its growth. For example, it would make it more difficult for matters to create biofilm.

The morbus Kostmann causes a lack of production of LL-37 in the granulocytes and in the saliva, the death from bacterial infection is almost completely certain within the first year of life if there is no immediately treatment with cytokine G-CSF [22], [23].

At certain concentrations, the LL37 peptide can also be toxic, for example strong hemolysis has been found at concentrations slightly higher than that necessary for bactericidal action (MIC, Minimum Inhibitory Concentration). However, LL37 peptide has not only bactericidal property but also fights against the side effects of the infection thanks to the ability to bind to liposaccharides (LPS). During a serious infection, Gram-negative bacteria secrete a high amount of LPS an endotoxins. LL37 can bind to the LPS or to a receptor downstream of the signal that inhibits the association between LPS and its receptor, reduces their action [14]. The interaction varies according to the type of bacterium, in Gram-negative bacteria the first approach takes place with the oligosaccharide chains present in the external wall while in Gram-positive bacteria it is dictated more by the electrostatic attraction. Another regulatory action is given by the chemotactic properties of the LL37-peptide, it is in fact able to recall cells of the immune system to the infection site and to pilot some of these as for the degranulation of mast cells. The pro-inflammatory mediators are released in the surrounding tissue facilitating the arrival at the site of other cells through

the increase of vascular permeabilization [23]. Comparing it to antimicrobial activity, the chemotactic activity of LL37 is less successful due to the presence of human serum [14]. A key feature of LL37-peptide, which arouses a lot of interest in tissue engineering studies and applications, is the role it plays in wound healing. In addition to playing various roles in the fight against infection, LL37-peptide also acts as a promoter of reendothelization by pushing the keratinocytes to migrate along the edges of the wound in order to close it [24]. It also has a role in angiogenesis which could be fundamental in the formation of an extended tissue. To date, the most common use is for the repair of infected wounds or chronic wounds. This type of chronic wound is often subject to bacterial infections, another problem is that the altered blood circulation of the diabetic patient does not facilitate the work of systemic antibiotics. LL37-peptide and its topical administration is a great hope in this field of research [25].

The function of LL37 depend through interaction with cell membrane or through receptors. In our study, for instance, we researched one of the receptors that was known in the literature for its connection with LL37-peptide, EGFR (endothelial growth receptor factor). Direct interaction has also been demonstrated with P2X7 (which play a role in neutrophil apoptosis, this is an important factor in the fight against the invader [14]), FPRL-1 (which mediates angiogenesis) and TLR (Toll-Like Receptor).

Recently it has been thought to use LL37 also as an anticancer agent but its modulating action varies according to the cancerous phenotype and its original tissues [14]. however, the inhibition or promotion of tumor growth by LL37 have been found, and therefore the details studies are required to understand the mechanism [26].

### **6.1 Role in odontogenic regeneration**

Some studies have shown a correlation between LL37 and bone growth. LL37 peptide differentiates mesenchymal stem cells (MSCs) to bone like cells which is characterized using alkaline phosphatase and mineralization assays. In particular, mouse MSCs (mMSC) have been tested and an improvement in proliferation, bone differentiation in terms of increased mineralization and alkaline phosphatase activity has been noted [27]. In another study, a fragment of LL37, called KR-12, was used on HBMSC (human bone marrow stem cells); dose-dependent activation of transcription of bone morphogenetic protein 2 (BMP2) through BMP / SMAD signaling has been demonstrated [28]. The regenerative potential of LL37 has also been studied on human stem cells of the dental pulp (hDPSC). The result suggests

that LL37 plays an active role in odontogenic repair even in the absence of ostioinductive substances in the culture environment [29]. In the stem cells of the apical papilla, the expression of the osteogenic gene is downregulated in the presence of bacteria or biofilm and consequently a decrease in mineralization is noted [10]. In our project the ability of LL37 to stop the infection and promote bone regeneration has been exploited, the SCAPs in contact with the peptide undergo a differentiation towards the odontogenic phenotype.

## **7. Nanoparticles**

Nanotechnologies are today a means to break down the limits that medicine placed in the past or, in any case, an improvement in the specificity, timing, and effectiveness of existing treatments. In this study the multi-functionality of gold nanoparticles coated with LL37 peptide is explored as antimicrobial and differentiating agent of stem cells. The functionalities, antimicrobial and differentiators ones, are inherent in the peptide but the gold nanoparticle formulation increases and improves its efficiency. Nanoparticles are widely used in modern medicine for their characteristics, the most evident is certainly their size (from 1 and 100 nm) and their large surface area to volume ratio that allows them to better interact on a cellular and subcellular level then depending of the material they assume many other characteristics [30]. At the same time we also want to be able to direct the NPs and to see where they are. In most cases we are interested in combining, transporting and releasing a drug to specific sites or the particle itself with its material and size can be used both in therapy and in diagnostics. For example, they can be biosensors and at the same time controlled drug release platforms or contrast and heat-abating agents. The goal of today's medicine is to seek increasingly complete, versatile and specific solutions for the patient or the disease treated; there is consideration of theranostic nanoparticles [31]. In the case study, gold nanoparticles conjugated to the multifunctional peptide LL37 were used. Metallic nanoparticles (iron oxide or titanium, gold, silver) are interesting for their optical and magnetic properties; they are also used for imaging. Metals, such as silver or copper, are used as additive antimicrobial agents. [32]

### **7.1 NPs in dental applications**

Nanoparticles are widely used in the dental field. This branch is called nanodentistry [33]. The applications range from the most common aesthetic treatments (whitening) to adhesive pastes for dental prosthesis up to the nanoparticles used in endodontics. Many of the techniques used in dentistry



generate narrow cavities, places easily colonized by the microbiota that naturally resides in the oral cavity. Compared to traditional antimicrobial agents, NPs have better ability to interact with microbes and any drugs they carry are better stabilized. The antimicrobial effect obtained with a nanoformulation is more effective in the long term. Silver has antimicrobial properties against a large number of microbes, including antibiotic-resistant strains, and for this reason many studies rely on the use of silver nanoparticles (AgNPs). They are often inserted in materials for dental applications (toothpastes, composite resins, cements and implant coatings). The bactericidal action is due to the  $\text{Ag}^+$  ions that are released, therefore it increases as the size of the nanoparticles decreases ( $<10\text{nm}$ ). They are able to damage/oxidize the membrane of bacteria and interfere with the production of ATP, DNA replication and the formation of reactive oxygen species. Likewise, being in contact with host cells, they are potentially toxic. Many studies reveal oxidative damage to organelles and massive accumulation in the liver, for this reason AgNPs are usually incorporated into polymeric matrices. They are also proposed as an irrigant to disinfect the root canal and as an additive for gutta-percha. As a coating of titanium implants, AgNPs have promoted the bone growth necessary to avoid movement. This can be attributed to the formation of microgalvanic couples between the two metals. AgNPs are proposed as blocking agents of the crack in the dental porcelain, even if the aesthetics are affected, this fine nanoparticle dispersion increases the mechanical properties of the ceramic. It is necessary to know the long-term effects in vivo [34].

Some researchers have analyzed a treatment similar to that proposed in this thesis work. They studied the effect of a laser on nanoparticle irrigants (AgNPs and AuNPs) in endodontic applications. This combined effect has been shown to provide purchasable results with usual disinfectants. In the case of AgNPs they are even better [35].

Other nanoparticles that have shown antimicrobial effects are zinc oxide nanoparticles (ZnONPs), chitosan nanoparticles (CS-NP) or a combination of the two (ZnONPs coated with CS multilayer). Zinc oxide is a strong antioxidant, it avoids recolonization, while chitosan is a very versatile hemostatic polysaccharide. Among the polymeric antimicrobial nanoparticles, poly(lactic-glycolic) acid (PLGA) NP nanoparticles loaded with methylene blue (MB). MB is a

photosensitizer and reacts to red light (665nm), this formulation could be a model for the encapsulation of photoactive drugs (photodynamic therapy (PDT)) but the presence of serum proteins limits its action. The ability of cationic chitosan NP to interact with bacterial cell surfaces and photoactivation of RB (photosensitizing rose bengal) have been combined into a single antimicrobial nanoformulation. Finally, various materials based on calcium, phosphate, silicates etc. have been used as nanocarriers for antibiotic drugs (such as Tetracycline) but in the long term with the slow release of ionic compounds. An example can be the bioactive mesoporous calcium – silicate NPs. They are designed to be injected and, thanks to their pore volume and high specific surface area, they could be used as a filling agent of the apical root canal [33].

About 60% of dental restorations fail for two reasons: secondary caries and bulk fracture. To improve these treatments, composite materials with antimicrobial and self-repairing functionality of the crack have been proposed. To repair the cracks various microcapsule systems have been proposed. In one study, microcapsules containing a reparative agent that is released and activated if affected by the crack. In this case, the role of the nanoparticles of amorphous calcium phosphate (NACP) is to mineralize the matrix, the antimicrobial role is entrusted to the dimethylaminohexadecyl methacrylate (DMAHDM) [36].

## **7.2 Gold NPs**

From the historically proven use of gold in medicine [37], we can consider gold a biocompatible and inert material, moreover it is easy to synthesize and functionalize. Gold nanoparticles (AuNPs) are presented in the form of colloidal suspension. AuNPs are formed by reduction method in the presence of a stabilizer, chloroauric acid and trisodium citrate [31]. Depending on environmental conditions, such as temperature and the composition of the reaction medium (that determines the pH), The size and physic-chemical properties of AuNPs change according to the shape such as, hexagonal, rod, hollow or solid NPs. Nanorods are used for photothermal therapy and cancer imaging [38]. Often PEGylation is used to increase the half-life of the NPs in blood circulation system. In our case, PEG coated AuNPs were considered the negative control. Amino acids or peptides are used to do specific targeting or to increase the internalization of NPs. NPs functionalized with DNA sequences or antibodies are mostly used as sensors [31].

Immobilization of biomolecules is achieved by various techniques including: physical adsorption, electrostatic bonding, specific recognition and covalent bonding. More often the non-covalent bond is used to avoid altering the structure of the biomolecule [37]. Other common applications of AuNPs are: the gene or drug delivery, increasing the permeability in the membranes (also towards bacteria), diagnostic and therapeutic cancer agents (through the enhanced permeability and retention (EPR) effect and the overexpression of the cancer cells), photothermal ablation, bioimaging and much more.

AuNPs have been used to develop molecular diagnostic biosensors using the detection of a refractive-index change [39]. Depending on the size and shape, the color and the optical properties of AuNPs are changed [40]. Cancer, the plague of our century, it is commonly treated with radio- and chemo-therapies that involve damage to healthy tissues, with nanotechnologies EPR and specialized targeting are used to target only cancer cells. This characteristic of gold nanoparticles, LSPR, is exploited in Photothermal therapy (PTT), the NPs internalized in the tissues and cancer cells are excited with radiation in the specific band and releasing vibrational energy and therefore heat kill the target cells [41]. AuNPs are also used as a contrast agent during diagnostic or surgery phase, photoimaging allows to identify well the edges of the diseased tissue and offers a much higher resolution of the techniques used today (MRI and CT) in order to identify a tumor in the state primordial [41]. In this project, the use of LSPR is proposed to damage bacterial membranes and thus increase the internalisation and bactericidal action of LL37-AuNPs, a green laser was used for this purpose (wavelength 535nm, power of 0,5 W/cm<sup>2</sup>) to excite the free electrons of the nanoparticle.

Some studies have shown that gold nanoparticles are able to direct the differentiation of MSCs, to act on their proliferation and mineralization. It is also known that the shape and size of AuNPs are influenced by the timing and quality of differentiation. It was demonstrated that, by activating the p38 mitogenase and therefore the pathway of the mitogen-activated protein kinase (MAPK), the NPs regulate the expression of the genes of osteogenic differentiation and inhibit adipogenic differentiation. This behavior is both dose and time dependent [42]. AuNPs can be internalized with various processes (pinocytosis, phagocytosis, endocytosis, clathrin-mediated endocytosis and caveolae-dependent endocytosis)

acting as mechanical stimuli on the MSC. They activate the mechanotransduction by regulating the activation of Yes-associated protein (YAP) [40]. The arginine-glycine-aspartate (RGD) adhesive peptide can bind to the integrins present on the cell surface and trigger some reports. In one project it was shown that high densities of this peptide on AuNPs lead to greater internalization but that this can inhibit osteogenic differentiation preferring adipogenic one. The low focal adhesion and stress of the cytoskeleton, in fact, push the MSCs in the adipogenic direction [43]. A study on dental calcium phosphate cement (CPC) loaded with AuNPs improved the osteogenic differentiation of hDPSC [44]. This is an excellent example of tissue engineering: the CPC is injectable (allows the filling of complex shapes), macroporous (allows the seeding and cellular diffusion), once hardened it supports the loads and is ostioinductive. In the study cited, AuNPs increase cell adhesion, proliferation and ostiogenic potential without changing the mechanical properties of the structure, the two materials work synergistically, and the effects of the direct addition of AuNPs in the culture media of hDPSC were tested and it turned out that the action was the same but faster as the nanoparticles did not have to be released from the scaffold.

### **7.3 LL37-AuNPs**

AMPs are formidable antimicrobial agents and a possible breakthrough in the fight against the relentless development of resistance by pathogens. In testing the endogenous use of these antimicrobial peptides there are some difficulties: they are not stable in the serum and are degraded by proteolytic enzymes. To compensate for this deficiency, it has been tried to use high concentrations which, unluckily, are cytotoxic and hemolytic. Nanomedicine can help overcome these obstacles. In many articles it is shown how stabilized these molecules by resorting to drug release systems but once released it returns to the usual problems listed above [45]. One possibility, which can solve all the stability problems, is the immobilization of the peptide through covalent bonds. In some studies, it has been proven that the biological characteristics of the AMP remain even after binding. There is more antimicrobial and targeting activity than free peptide [46]. Antimicrobial activity depends on a series of factors to consider when making a formulation such as the arrangement of the peptides, the packaging and therefore the density, their length

and their flexibility. The charge that makes them prey to plasma proteins is also very important [45].

There are several possible binding methods, but they are often long and the procedure changes depending on the peptide used. In other works, for instance, CM was immobilized on gold-covered magnetic SPIONs [47] and on surfaces coated with gold nanoparticles [45]. AMPs have also been immobilized on polymers and other metals.

In this thesis work a method has been used that allows to synthesize gold NPs directly functionalized with the AMP called one-step synthesis. The technique has been described in a study where AuNPs were synthesized using the CM-SH peptide as a capping agent. CM-SH is a CM (cecropin-mellitin) to which a cysteine has been added, this provides a thiol group (-SH) capable of binding the gold surface and limiting the action of piperazine ring in HEPES. HEPES is an agent that can reduce AuCl<sub>4</sub> to AuNPs very quickly and in an uncontrolled way [46], so we need a capping agent.

The same synthesis procedure was also carried out on other AMPs such as Magainin-1, Tet-20 and, as in our case, LL37 [48].

LL37 has been successfully immobilized on gold nanoparticles by a one-step procedure [46].

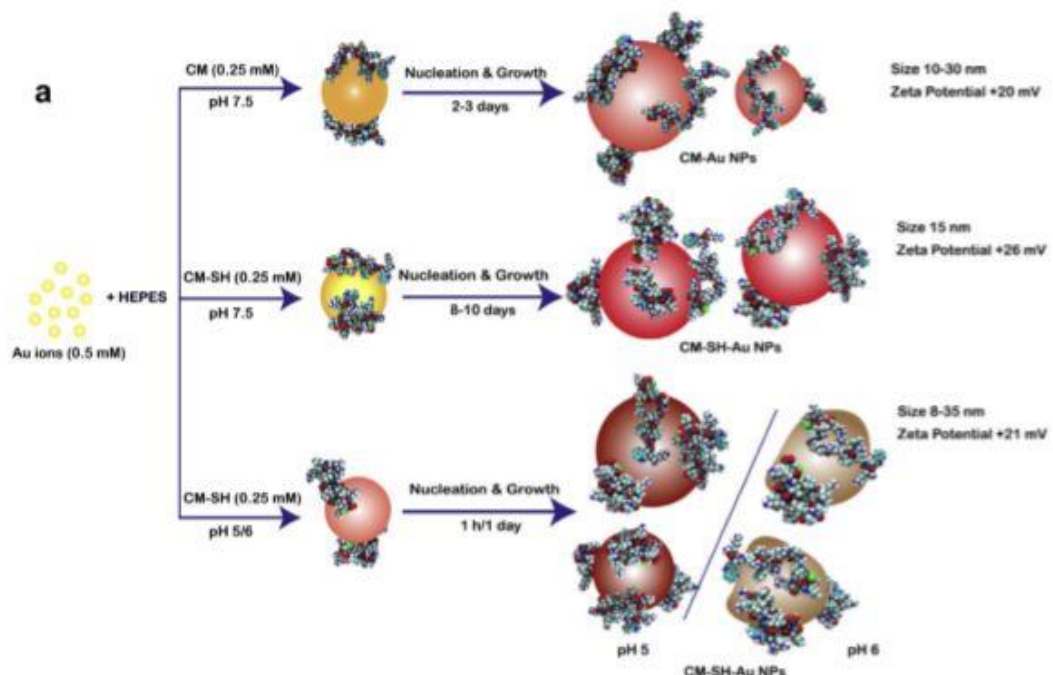


Figure 6-different experimental conditions of synthesis of Au NP in the presence of a peptide (CM) [46].

This formulation has already been shown to increase the antimicrobial and pro-regenerative potential of the skin both in vitro and in vivo. It increase the expression of collagen, IL6 (interleukin-6) and VEGF (Vascular Endothelial Growth Factor); prolong the phosphorylation of EGFR and ERK1 / 2 (Extracellular signal-regulated kinases); they stimulate the migration of keratinocytes through P2X7 receptors and the transactivation of EGFR. The platform has therefore extended the bioactivity of the AMP by stabilizing it against the inactivation of the serum and proteolytic degradation [24]. Many drug release systems are based on the diffusion of the molecule, in the case study the chemical immobilization allows to control the density and spacing of the ligands, the size of the nanoparticles and therefore the bioactivity of the molecule.

#### **8. Aim of the project**

The aim of this project is the creation of a multifunctional platform capable of eliminating and preventing infections and at the same time stimulating the reconstruction of the pulp chamber. In endodontal operations, the vitality of the tooth is often lost as the root cannot remain exposed to infections, there is a risk of bacteria spreading throughout the body. With the help of LL37-AuNPs the infection could be eliminated and the tooth could self-heal by exploiting the MSCs cells present in the apical part of the papilla (SCAPs). The differentiation and antimicrobial properties of LL37-peptide are amplified in the nanoformulation compared to AMP in solution [48]. If conjugated it interacts better with both the bacterial and the cellular membranes of the SCAPs. Furthermore, the properties of the base material of the formulation and therefore the physical phenomenon of local surface plasmonic resonance have been exploited to increase its bactericidal effect.

## Materials and methods

### 1. Materials

All materials, tools and work facilities were supplied by UC-Biotech and Matera in the Biocant technology park, Cantanhede, Portugal.

The peptide (LL37 modified with a C-terminal cysteine, Caslo laboratory, Denmark) was purchased lyophilized, 96% purity. The peptide is the result of various steps: conventional solid phase synthesis, purification by high performance liquid chromatography (HPLC) and characterization by mass spectroscopy at matrix assisted ionization time with laser desorption (MALDI-TOF).

HAuCl<sub>4</sub>·3H<sub>2</sub>O (chloroauric acid trihydrate), DMF (dimethylformamide, HCON(CH<sub>3</sub>)<sub>2</sub>), sodium citrate (Na<sub>3</sub>C<sub>6</sub>H<sub>5</sub>O<sub>7</sub>) and PEG (Polyethylene Glycol) were used as received (Sigma-Aldrich).

For the one-step synthesis of nanoparticles, we need to prepare the 100mM HEPES buffer (4-(2-hydroxyethyl)-1-piperazineethanesulfonic acid, Sigma-Aldrich) at established pH. HEPES is a zwitterionic sulfonic acid sold in powder (238Da) and is used for its ability to maintain the pH value. Assuming to prepare 100ml of them, we weigh and dissolve 2.38g in 100ml of milli-Q water and maintain the pH 5.

Various bacteria and culture media have been used in antimicrobial tests:

- *Escherichia coli* (*E. coli*), *Staphylococcus aureus* (*S. aureus*), *Enterococcus faecalis* (*E. faecalis*), *Staphylococcus epidermidis* (*S. epidermidis*) and *Escherichia coli* ML-35p (*E. coli* ML-35p) were purchased from DSMZ, German Collection of Microorganisms and Cell Culture. Dyes such as Nitrocefin and ONPG (o-nitrophenyl-3-D-galactoside) were used in the permeabilization test. Adult male Human Serum was purchased from Invitrogen.
- All culture media were made following the manufacturer's instructions. Plates of TSY-Agar (Trypticase soy-Agar) and BHI-Agar (Brain-Heart infusion broth-Agar) were made. The sterilized liquid media (maintained at about 60°C after sterilization) were poured in sterile Petri dishes and left to the cool/solidify in the biological hood. Agar is used as a support in semi-solid culture media and solidifies below 50°C. The same procedure, unless the Agar, was followed to make liquid TSY which is simply sterilized and brought to room temperature. Liquid BHI was bought from Frilabo.

The green laser is from Changchun New Industries Optoelectronics Technology Co., model MGL-N-532nm-3W-19012955(PO#54). Before use it is necessary to wear gloves, green light filtering glasses and stabilize the instrument for 10min.

The cells used, SCAPs (stem cells from the apical papilla), come from The Center for Neuroscience and Cell Biology (CNC), Coimbra, Portugal. For the cultivation two types of media were used. They are made by filtering the different components, in a biological hood, so as not to incur contamination:

- maintaining media composed of: 1% V/V of GlutaMAX 100x (Gibco), 1% V/V of  $\beta$ -mercaptoetanol 10mM (Sigma-Aldrich, diluted in PBS), 1% V/V Pen / Strep 100x (Penicillin Streptomycin Solution), 20% V/V of FBS-HI ( Heat-Inactivated Fetal Bovine Serum, 30min in a water bath at 56°C), the remaining volume is KO-DMEM (KnockOut-Dulbecco's Modified Eagle Medium, Gibco)
- odontogenic media composed of the same basic elements in the same concentrations but with additional components necessary for differentiation. The new components are: 10 nM dexamethasone (Sigma-Aldrich, solubilized in ethanol and then diluted in KO-DMEM), 10mM  $\beta$ -glycerophosphate (Sigma-Aldrich, solubilized with KO-DMEM) source of organic phosphates, 50 $\mu$ g/mL ascorbic acid (Sigma-Aldrich, solubilized with KO-DMEM) [27].

In some experiments, a much simpler culture medium consisting of only KO-DMEM and 1% V/V Pen / Strep was used to eliminate the influences of the additional components.

The test to avoid the presence of mycoplasma was carried out following the instructions of the *MycoAlert kit* (Lonza) on a sample of culture medium used during cell expansion.

*CellTiter-Glo® Luminescent Cell Viability Assay* was used for the cytotoxicity test.

The *BD Accuri C6 benchtop flow cytometer* from *BD Biosciences* (San Jose, CA) was used for EGF receptor research.



Figure 7-BD Accuri C6 benchtop flow cytometer [68]



*IN CELL Analyzer 2200* (GE Healthcare Life Sciences) was used for the acquisition of images aimed at evaluating cell proliferation.

For the ALP and mineralization tests the following were prepared:

- blocking solution of the reaction induced by *1-Step PNPP* (p-nitrophenyl phosphate disodium salt, Thermo Scientific), then 2N NaOH (Sigma-Aldric; 0.8 g of NaOH in 10ml of milli-Q water)
- formaldehyde solution (Sigma-Aldric) to fix the monolayer, 10% V/V in milli-Q water
- 40mM solution of Alizarin Red (Sigma-Aldric) (1.37g per 100ml of milli-Q water), was then brought to pH 4.1 using ammonium hydroxide (10%V/V) or hydrochloric acid.

## 2. Nanoparticles preparation

In this thesis work a method has been used that allows to synthesize gold NPs directly functionalized with the AMP called one-step synthesis.

LL37-Au NPs were made following this protocol [48]:

- LL37-peptide with a cysteine at C-terminus (4490Da) is weighed, which is in powder form, and is dissolved in a minimum quantity of DMF (2.0mg in 100  $\mu$ l). Then, this solution is diluted in 900  $\mu$ l of HEPES. The final concentration of LL37-peptide will be 2mg/ml (0.5mM)
- the aqueous solution of gold ions is made by diluting a  $\text{HAuCl}_4 \cdot 3\text{H}_2\text{O}$  (chloroauric acid trihydrate,  $10^{-2}$  M) solution in milli-Q water
- The final concentration should be 0.5mM of gold ion solution (50 $\mu$ l in 1ml of solution) and 0.25mM of peptide solution (562 $\mu$ l in 1ml)
- the remainder will be HEPES (388 $\mu$ l in 1ml), it is important to add the gold solution as the last reagent, since when we add the gold ions in the HEPES buffer the reaction takes place and we are no longer able to bind the peptide.
- The reaction takes from 4h up to a week in a 25°C water bath, the time will depend on the pH of the buffer (5 to 7,5); at the end we would have a red-violet suspension of LL37-AuNPs
- to isolate the NPs, proceed with the centrifugation (11000rpm for 10min at 4°C). Then the supernatant is removed and the nanoparticles are resuspended in milli-Q water. If

the supernatant is still light red, repeat this step on it with higher speed (14000rpm for 10min at 4°C)

- to know the real concentration of our suspension of LL37-AuNPs, we proceed with the freeze-drying of a known aliquot in volume. The small volume of NP solution was taken in a perforated tube (for depressurization), freeze at -80°C the necessary time and put it in the freeze dryer. By calculating the net weight and knowing the initial volume, we are able to calculate the concentration of the entire preparation in terms of mg/ml
- In the case of biological use, as in our case, it is necessary to sterilize this suspension (30min of exposure to UV lamps into a biological hood)
- store at 4°C for non-immediate use

The procedure just described is the result of an optimization made in a previous work [48] and leads to the synthesis of LL37-AuNPs (pH 5) with high density of AMPs (approximately 154 peptides per NP), with low polydispersity and dimensions of the average diameter at 20nm ( $21 \pm 8$  nm), with positive charge ( $+ 15.4 \pm 2$  mV). We used LL37-AuNPs (pH 7.5) which have a diameter ( $12 \pm 3$  nm) and a Z-potential of  $-3.5 \pm 1.1$  mV. The same study shows how, despite the immobilization of the peptides eliminates the secondary helical structure, the antimicrobial characteristics of the bound peptide are maintained and there is no sign of leaching.

For the control, PEG-coated gold nanoparticles (AuNPs) have been made using Turkevich method (gold NPs) followed by PEGylation of Au NPs. The Turkevich method uses sodium citrate ( $C_6H_5Na_3O_7 \cdot 2H_2O$ ) as a reducing agent, then the citrate ions are adsorbed on the spherical surface created and, being negatively charged, thanks to the electrostatic repulsion they prevent aggregation. We thus obtain a colloidal suspension of spherical AuNPs.

PEG (Polyethylene Glycol) is an inert and hydrophilic polymer widely used in the pharmaceutical field for various properties among which we find: the increase in solubility and stability, the reduction in immunogenicity and antigenicity, increase in the half-life of the object in question. it is able to make nanoparticles/molecules invisible to the immune system. In this work, PEGylation (i.e. the PEG coating) was used to stabilize the Au NPs.

AuNPs were created with the following protocol:

- a magnetic stirrer is set at a temperature of about 100°C, with a probe thermometer we check the temperature. Using an Erlenmyer flask, we begin to homogeneously heat 90ml of milli-Q water
- we want to obtain a concentration of HAuCl<sub>4</sub> 1mM, add 1ml to the flask of HAuCl<sub>4</sub> solution (0.1M)
- 10ml of milli-Q water are then used to dissolve 0.2g of sodium citrate, sonicating can help the dispersion.
- Once boiling, the reducing agent is carefully added. In 2-3 minutes we can observe the change of solution for transparent to ruby red.
- The solution is allowed to cool and then is PEGylated. 1mg of PEG is added to each 40ml of gold nanoparticles, allowing the reagents to interact for a few hours.

### 3. Bacterial culture

In order to give completeness and generality to the experiment it is important to test antimicrobial activity against both Gram-negative and Gram-positive bacteria. Different bacteria have been used: *Staphylococcus aureus*, *Enterococcus faecalis*, *Staphylococcus epidermidis* and *Escherichia coli*. In the root canal space, the most common bacteria are *S. aureus* and *E. faecalis*. The bacteria are stored in the laboratory by freezing them. To start the bacterial culture, a small amount of bacterial solution must be defrost and re-cultivated on a Petri plate of TSY-Agar or BHI-Agar. After 12 or 24 hours in an incubator at 37°C, depending on the type of bacteria, colonies of bacteria will appear on the plate. The first cultivation phase is on the plate. The isolation of individual colonies (group of individuals deriving from the same progenitor) is desired. The first dilution is made by drawing a zig zag with a loop (flame sterilized, cooled and put in contact with a colony) on the plate. One takes an angle from this and, with the same movement, the bacterial load is still diluted and so on until the third dilution. After 12, 24 or 36 hours in the incubator we obtain the single colonies, at this point we can use or stop their growth at low temperature to preserve them. The second culture phase occurs in suspension. The single colony is transported in about 5ml of culture medium (TSY or BHI) and stirred at 150 rpm and at 37°C. By shaking the suspension, the interaction between the peptide/NPs and the bacteria is simplified, avoiding sedimentation [49]. Each strain has different growth rates. To obtain bacteria at their maximum activity, they have to be used when they are in the exponential phase. To know the state of growth of the bacteria in basic suspension is the visual inspection, the solution becomes turbid, but it is a first qualitative evaluation. Quantitatively the absorbance at

600nm is calculated, so 200µl of bacterial suspension in a well of non-opaque 96-multiwell plate are read with a spectrophotometer plate reader and Gen5 software. An absorbance value of about 1 is considered adequate ( $OD_{600}=1$  is equivalent to  $2 \times 10^8$  cfu). From the absorbance value it is possible to deduce the concentration thanks to a known calibration curve. At this point, the first dilution in PBS of  $10^8$  cfu/ml (colony forming unit per milliliter) are made and from this a series dilution is carried out until reaching the desired concentration for the test (in PBS or 10% V/V HS).

### 3.1 Green laser

Green laser with CW(Continuous-Wave) operating model at 532nm and maximum power of 3.32W, emitted through an optical fiber of a meter whose lens is positioned at 7 cm from the base. The cross-sectional area of the beam is about  $1.5 \text{ cm}^2$ .

The power after passing through the optical fiber becomes 2.08W [50], so it is smaller.

The laser is produced by a semiconductor which, subjected to a potential difference, allows the doped p-n transition. From the recombination of an electron with a hole, a photon is spontaneously generated. This energy varies according to the material. As well known, energy is associated with a wavelength and therefore a color. In the laser this coherent radiation is maintained. In particular, in this project a laser DPSS was used which exploits an infrared GaAlAs laser diode pumps with neodymium-doped yttrium aluminum garnet (Nd: YAG) crystal which produces 1064 nm wavelength. Using a KTP crystal the nonlinear optical process doubles the frequency by dividing the beam and then obtaining 532 nm light [51].

The combination of laser and Au NPs creates the so-called LSPR (Localized Surface Plasmon Resonance). In this physical mechanism the metallic nanoparticles, if exposed by radiation at a given wavelength, are able to accumulate energy and then release it in the form of thermal energy to return to a state of no excitement. We use the green laser because the Au NPs (average diameter of about 20-30nm), due to the plasmonic resonance phenomenon, absorb the blue-green light depending on the size.

In this work the thermal energy generated by AuNPs after exposure of laser light is used to damage the cell membrane and thus allow the LL37 peptide to increase its bactericidal efficiency. In the tests a low power density was chosen ( $0,5 \text{ W/cm}^2$ ) and a limited time (1min). The single exposure didn't make much difference, so we

thought about a longer exposure. In order not to risk overheating of the solution and since in some articles it is evident that a pulsed administration increases the plasmon resonance effect, we have chosen to follow a protocol that alternates three exposures of 1min to 10sec of relaxation. The particles do not have time to release all the energy that are excited again multiplying the effect.

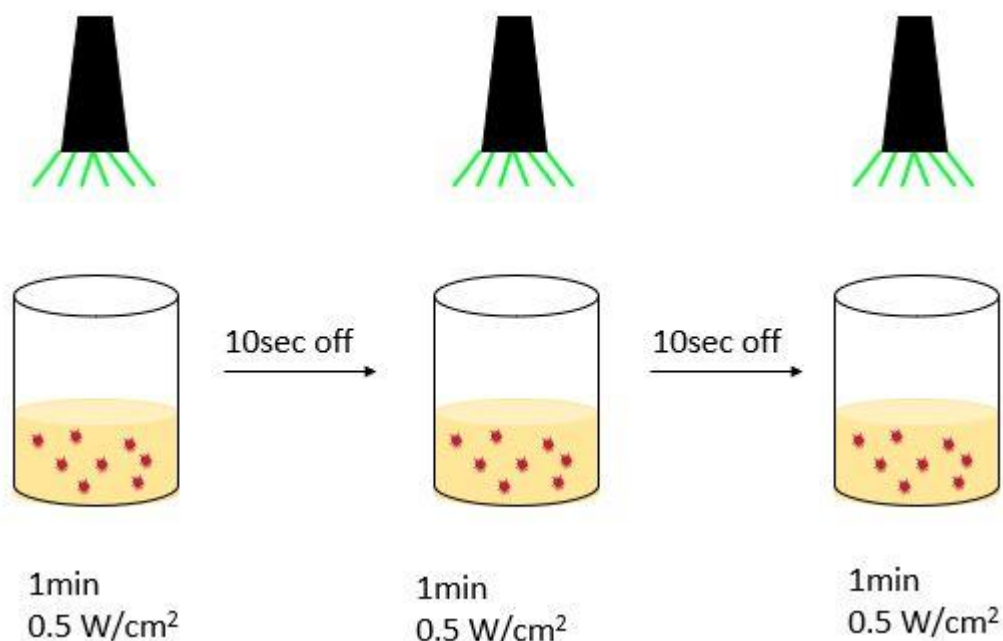


Figure 8-Procedure scheme for green laser exposition

### 3.2 Antimicrobial test

To test an antimicrobial agent, reference is made to parameters. The most used parameters are IC<sub>50</sub> and MIC. The IC<sub>50</sub> (half-inhibitory concentration) identifies the concentration at which 50% of the inhibition occurs while the MIC (minimal inhibitory concentration) is defined as the lowest concentration which allows to obtain zero bacterial growth.

To determine the antimicrobial potency of an agent, various tests exist such as the diffusion, the evaluation of turbidity, the enzymatic, potentiometric and radioimmune assays [52]. In the case of antimicrobial peptides, the broth microdilution test was affirmed, which provides the MIC. Essentially, the bacterial culture is subjected to treatment at various concentrations. The bacteria grow in wells of a 96-multiwell plate which acts as a support for the spectrophotometric. The reading at 600nm is carried out

during a certain incubation period [49]. The turbidity of the bacterial suspensions in the wells is already a visual index of bacterial growth but is finely quantified with spectrophotometry. Different culture media can be used depending on the type of bacterium and the stability of the tested antimicrobial agent. As far as peptides are concerned, a significant sensitivity to serum degradation was found [52]. For this reason and for the obvious application needs, the broth microdilution test was carried out in this project in human plasma. This method does not allow to distinguish between a bacteriostatic and bactericidal effect, that is, if growth is stopped or if bacteria are actually killed. To understand if there is a bactericidal effect, it is necessary to refer to another index called minimum bactericidal concentration (MBC), to calculate it the plate counting method is useful [49]. In our experiments the combination of these two methods was used [47] [46] [45].

Preliminary tests involved one of the most common bacteria, *Staphylococcus aureus*. Several antimicrobial tests have been taken into consideration. What proved to be the most suitable for our test was Broth Microdilution Antibacterial Assay [52]. From the first dilution in PBS of  $10^8$  cfu / ml, a series dilution is carried out until reaching the concentration  $10^6$  cfu / ml in PBS. We observe the behaviour of the solutions at  $10^5$  cfu/ml concentration in every condition at time zero and in the following 24 hours with time point at 5h and 24h. The spreading and plate counting method is used to show the results. This method involves dispersing 50  $\mu$ L of bacterial suspension on an Agar petri dish (TSY or BHI) and letting it grow for at least 24 hours in order to visualize the bacterial colonies present. To make the count possible the culture concentration  $10^5$  cfu / ml is still too loaded; its dilutions  $10^4$  cfu/ml and  $10^3$  cfu/ml in PBS are used, in this way the colonies are in the range of hundreds and are easy to distinguish. Each condition is tested in triplicate to have statistical relevance. In the first experiments a culture medium unfavourable to bacteria (PBS) was used, while later on we tried to understand if, in the presence of nutrients and in conditions more similar to those of a future use of the tested material, it would have worked the same way. To this end, human adult male serum (HS) at 10% V/V (in PBS) was used.

Synthetically summarizing the steps for antimicrobial tests, we find:

- culture in suspension overnight
- absorbance reading at 600nm with spectrophotometer and Gen5 software
- determination of concentration through calibration curve

- serial dilutions up to  $10^5$  cfu / ml with various conditions
- laser exposure
- spread of  $10^4$  cfu / ml and  $10^3$  cfu / ml dilutions at time points (0h, 5h and 24h)
- colony count after 24h

Through the dilution ratio, it can be traced back to the actual number of colonies present and viability can be calculated. For example, if we have plated 50 $\mu$ l of 1ml of bacterial suspension  $10^3$  cfu/ml we have a dilution factor of  $20 \times 10^2$ .

### 3.3 Bactericidal mechanism: permeabilization

A colorimetric test is used to understand how each component contributes to the bactericidal action. The bacterium *E. coli* ML-35p is engineered to be constitutive for cytoplasmic  $\beta$ -galactosidase, lacks lactose permease, and to express a plasmid-encoded periplasmic  $\beta$ -lactamase [53]. Two different molecules are used. They act as a substrate with two enzymes, one found in the membrane part and one in the cytoplasmic part of the bacteria. From the enzyme-substrate complex a molecule capable of coloring the solution is formed. So, the more the color intensity is high, more the enzyme is exposed and more the membrane is damaged. With the modifications made to the *E. coli* ML-35p we can distinguish which of the two cell membranes is being damaged (inner or outer) [45].

The dye for the outer membrane (OM) is Nitrocefin. The Nitrocefin is excluded from the periplasmic space where  $\beta$ -lactamase is found. When the OM is torn, the dye can cross it to be cleaved by the enzyme and produces a color change, it turns pink, that can be observed by spectrophotometer at 486nm.

Ortho-Nitrophenyl- $\beta$ -galactoside (ONPG) is a colorimetric substrate for  $\beta$ -galactosidase. *E. coli* ML-35p has no lactose permease, ONPG mimics lactose therefore cannot traverse its inner membrane (IM) to be cleaved. If the IM is pierced the ONPG cleavage produces a color change towards yellow, quantifiable at 420nm. The two wavelengths are too close together so to avoid spectrum overlap problems the two colors are evaluated separately. The experiment was designed to understand the importance of the LL37 peptide compared to that of the laser-AuNPs interaction. The conditions tested are:

- bacteria in contact with LL37-AuNPs
- bacteria in contact with LL37-AuNPs and subjected to the laser
- bacteria in contact with AuNPs
- bacteria in contact with AuNPs and subjected to the laser
- bacteria in contact with LL37-peptide
- bacteria not-treated.

In addition to the controls of bacteria with only the LL37 peptide in solution and only bacteria.

For each condition, two  $10^5$  cfu / ml bacterial solutions are prepared in 10% V/V human serum and the dyes are incubated. It is decided to do this last operation after laser treatment in order not to risk altering the dye molecules. The concentration of both dyes is known from the literature [53] (Nitrocefin  $30\mu\text{M}$  and ONPG  $2.5\text{mM}$ ). The dyes are dissolved in PBS. The tubes, with bacteria culture, placed in an orbital stirrer at 150rpm and  $37^\circ\text{C}$  are monitored for 24h, with an acquisition frequency of one reading per hour. The spectrophotometer readings were carried out by placing  $200\mu\text{l}$  of test solution in a 96 multiwell-plate.

#### 4. Cell culture

SCAPs are adherent cells and they need to adhere to a growing surface. In our experiments 6 or 24 wells tissue culture plates were used. The cells we use have been isolated from human pulp tissue, so it is possible to find a series of debris from the tissue in the culture. For the same reason, it is even more fundamental to verify the absence of mycoplasma. Cells are stored in liquid nitrogen at  $-195.79^\circ\text{C}$ , so the first step is the defrosting. 1ml of single cell suspension  $10^6$  cells / ml is heated, diluted in the culture medium, centrifuged at  $300\times g$ ,  $25^\circ\text{C}$  for 3min in order to aspirate the supernatant and resuspend the pellet, finally the cells are seeded in a culture flask for about 3/4 days. The first seeding is essential in order not to risk working with cells traumatized by thawing. Initially from a cryogenic vial (1ml,  $10^6$  cells / ml) with SCAPs in the third step (P3) were expanded to create all the cells (P4) used in our experiments, then they were frozen. It is important, in fact, to be able to compare the results so that the differences are free from extraneous factors. The cells are therefore from a single donor, having the possibility it would be better to maintain coherence on the passage but to test cells from different donors. Checking the cells, performing the mycoplasma test, changing the medium every 2/3 days are the basic



operations in a first phase in which the behaviour of the cells and their state of health are unknown. From our experience, one million SCAPs (P4) cells in a medium-sized flask (T75cm<sup>2</sup>) in 4 days, with a single change of culture medium after 48h, quadruple. Growth is also very fast compared to other types of MSCs [11]. When the cells in the flask reach a confluence of about 80-90% they are ready to be counted. Therefore, it is necessary to recreate the single cell suspension using trypsin, an enzyme that eliminates the anchoring of cells to the surface. More specifically, the culture medium containing a trypsin inhibitor is eliminated, the culture is rinsed in PBS and subjected to trypsin for about 3 min in an incubator. Centrifugation is carried out and then cells are resuspended in 1 ml of base culture medium. For the count a hemocytometer was used, 10µl of Trypan blue were mixed with 10µl of cell suspension (dilution 1:2) and 10 µl were inserted in the support slide. Trypan blue is a selective dye for dead cells, it cannot enter into cells with an intact membrane (it is called dye exclusion method). All visible cells within the four angular quadrants of a grid are counted under the microscope, averaged and multiplied by the dilution factor and the instrument factor (10000). At this point we are able to seed in a multiwell-plate according to the needs of the experiment. In fact, each type of cell has growth times, a certain size and different space requirements. In our case, the SCAPs immediately showed a fairly high proliferative rate which made it possible, following the indications of other research groups [11], to estimate the number of cells per well to be sown and the timing of adhesion and confluence.

#### **4.1 Cell viability**

Cytotoxicity test is important to understand the biocompatibility of NPs used for differentiation of SCAPs. We chose to make a quantitative test of cell viability based on the presence of ATP (adenosine triphosphate). The ATP is in fact a high-energy compound that serves the cell for storing the energy to be spent in all those reactions. So, the ATP is a signal of the presence of metabolically active cells.

The *CellTiter-Glo® Luminescent Cell Viability Assay* is composed of a substrate and a lysing buffer. The lysing buffer serves to break the cells and so to expose the content to the substrate that reacts in the presence of ATP to give the luminescence.

It initiates a mono-oxygenation reaction of Beetle Luciferin which becomes Oxyluciferin, this reaction in addition to the presence of molecular oxygen and ATP requires the presence of  $Mg^{2+}$  and a catalyst known as luciferase.

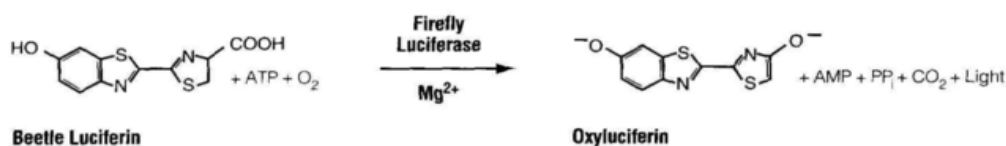


Figure 9-The luciferase reaction [66]

Thanks to this bioluminescence reaction, energy is released in the form of light. The emitted photons are detected with the aid of a spectrophotometer (gain 135, with a height of 1.25 mm).

First of all, it is important to understand the exact relationship between the luminescence values and the number of cells. It is therefore appropriate to start with a calibration curve. Simply knowing the number of cells used ( $0,5 \times 10^3$ ,  $1 \times 10^3$ ,  $2 \times 10^3$ ,  $4 \times 10^3$ ,  $10 \times 10^3$ ,  $20 \times 10^3$ ,  $50 \times 10^3$  cells/well) and calculating the relative luminescence values, we obtain a linear relationship ( $r^2=0,99$ ).

We then passed to the actual cytotoxicity test, we considered the LL37NPs and AuNPs nanoparticles in different concentrations ( $30 \mu\text{g/ml}$  and  $60 \mu\text{g/ml}$ ). As controls we used the LL37 peptide, mimicking the concentrations present in the LL37NPs (respectively  $8 \mu\text{g/ml}$  and  $20 \mu\text{g/ml}$ ), and the cells only. Each condition was replicated three times,  $20 \times 10^3$  cells / well were seeded in 24-multiwell plates. The protocol we followed involves eliminating the culture medium and washing in PBS, adding the same volume of reagent and culture medium ( $100 \mu\text{l}$  each on the 24-multiwell-plate), stirring for 20 min and letting the signal settle luminescent for 10 min at room temperature. Before obtaining the optimal setting of the experiment, various factors were varied including shaking time, gain (135 or 200), acquisition distance (1mm or 1.25mm) and stability over time by repeating the reading after 30min. As suggested by the manufacturer, the test is consistent only where the relationship is linear (below  $50 \times 10^3$  cells). Since between sowing, adhesion, treatment up to the test, about 48 hours pass and that we seed  $20 \times 10^3$  cells/well there was a risk of exceeding the linearity limit and so, to obtain real values, the samples were analyzed both as such and diluted by a factor of two.

## 4.2 Cell proliferation

To test the proliferative rate of the cells subjected to different treatments, we chose to use two dyes that mark the DNA but are not toxic at the concentrations used, this is because we want to analyze the same sample and how it varies over time. Hoechst stain fluorophores were used to observe the nuclei of living cells, and PI stain (Propidium Iodide), to observe the nuclei of dead cells or those that are starting an apoptotic process. In fact, PI is not permeable to healthy cell membranes. By doing both staining simultaneously we can observe the various cell states, this is necessary in the case of cells stressed by the treatments such as in cases where we use high concentrations of peptide or NPs. Being both linked to DNA if the cells were to proliferate with DNA, the fluorophore would also split and that's exactly what we need when we want to outline cell proliferation.

The two fluorophores can be used at the same time because they emit at two wavelengths far enough from each other to be well distinguishable, in fact we observe the Hoechst in blue-cyan (maximum emission at 461 nm) and the PI in red-orange (maximum emission at 636 nm). The conditions tested, in quadruple samples, are related to different concentrations of peptide (5, 10, 20 and 40  $\mu\text{l}$  / well), of LL37-AuNPs (30 and 60  $\mu\text{l}$  / well), of AuNPs (30 and 60  $\mu\text{l}$  / well) and the cells only.

The experiment requires less generous sowing in order to distinguish the nuclei well and prevent them from overlapping. However, if we wanted to maintain the same culture well format, 24 well-plates, we decided to seed 8000 cells / well, which is a slightly lower number than that optimized for cultivation ( $10 \times 10^3$  cells / well, i.e. about  $5 \times 10^3$  cells /  $\text{cm}^2$ ). This aspect is very important not only for easier viewing, especially for obtaining images more readable by the software used for quantization, IN Cell Analyzer.

As always, we avoid the immediate treatment of freshly seeded cells, after 24 hours from seeding in basic media, we proceed to treatment with peptide and NPs. In order to activate the pathway downstream of the interaction between peptide/NPs and cells, any other serum protein present in the basic media was eliminated, constituting a much simpler media based on KO-DMEM and Pen/Strep (1% V/V). By using this very poor nourishment medium the cells are stressed enough and this is why it was decided to limit the exposure time to only 4 hours.

In summary, 8000 cells / well are seeded; after 24 hours the basic media is eliminated, a PBS wash is performed, the cells are covered with the KO-DMEM 1% PEN/STREP and according to the tested condition also the NPs or the peptide are added; the treatment lasts 4h and at this point we can change the media by reinserting the complete one. The fluorophores were added according to the time points we need at a concentration of 0.25  $\mu\text{g}/\text{ml}$ . To obtain the complete staining, it is necessary to wait at least 20min.

In order to obtain convincing results we could not forget the potential cytotoxicity of dyes, for this reason we seeded several multiwells in order to stain the next day and after 5 days, comparing them we understood that the concentrations of fluorophores did not cause cell death. So, we found ourselves in the ideal condition to be able to analyze the same sample for all the duration of the experiment.

The analysis was carried out as IN Cell Analyzer 2200, an image acquisition system,

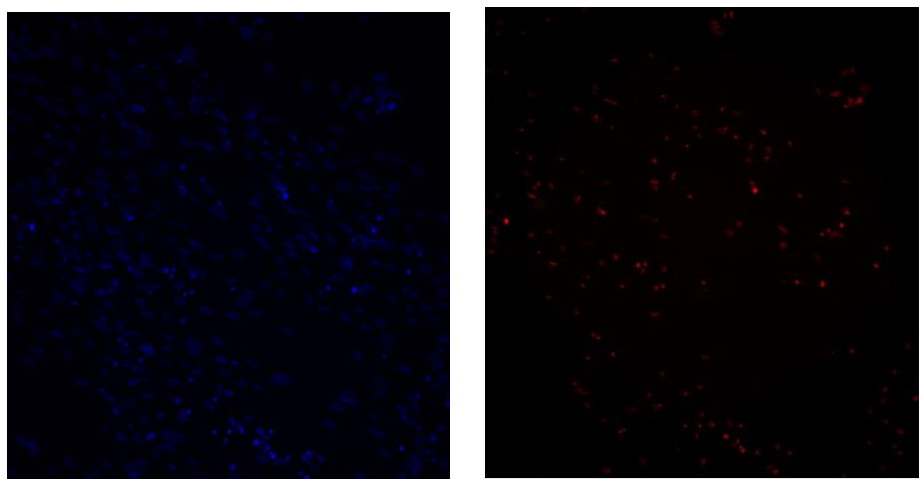


*Figure 10-IN CELL image of SCAPs after 48h from the treatment (only cells). The blue channel (Hoechst) are lived cells, the red channel (PI) are apoptotic or dead cells.*

and the associated software for post processing, recognition and counting of the two channels. Eight images are acquired for each well in fluorescence microscopy, the cells tend to be all in the center of the well so we avoid that area as well as that near the walls. Actually, each image is made up of three different acquisitions. Three channels were selected: TL-Brightfield (gray, showing morphology), TexasRed (red, dead cells) and DAPI (blue, live cells).

The large amount of images required the use of a software to count. The analysis was set up to divide the neighboring nuclei and, if the cell is stained with both dyes, it was counted as dead

### **4.3 Mechanism of interaction: EGF receptors**

For our study it is important to investigate the interaction between the free or bound peptide in the formulation with the cells, it allows us to understand how the therapy acts on the signaling level. In the case of LL37 peptide, among the various receptors certainly one of the most immediate to be searched is the EGFR (Epidermal growth factor receptor). EGFR is a transmembrane protein that specifically binds the factors of the epidermal growth factor family in the extracellular portion. Being a receptor, by binding to an EGF-like molecule, it produces signals inside the cell. Actually, it would not be the only access route for nanoparticles, but if there is a receptor, we are sure that the interaction will be specific and direct.

To observe the presence of the receptor a technique called indirect immunocytochemistry was used. The specificity of a primary antibody is used to mark the antigen which we are interested in, the EGFR. A secondary antibody recognizes the primary and carries with it a fluorophore that makes the binding site visible and therefore shows us the presence of the wanted molecule. In the specific case, when working with cells from human donors we used a primary antibody (rabbit anti-human) and a secondary Goat anti-rabbit IgG (Alexa Fluor 488).

As a detection method we have chosen to use flow cytometry which is a technology capable of counting single events in a flow. Therefore, it can count the cells and recognize if they are fluorescent marked because the machinery is based on optical technology.

The goal is to obtain a single cell suspension for each condition tested. First of all,  $400 \times 10^3$  cells / well were seeded in 6 well-plates, a high density is necessary because the samples will follow many steps and may not be significant enough for the statistics. As with any test performed, the cells are left to adhere for 24h and then the treatment is performed. In this case, it was preferred to test the treatment with peptide/NPs in the absence of other biosignals, i.e. using the medium without FBS (1%V/V Pen/Strep in KO-DMEM). After the 4h treatment, the complete culture environment was restored. The conditions were: the cells without any treatment (to understand if the SCAPs express this receptor), the cells subjected to the stress given by the poor culture medium, low concentrations of LL37-peptide (8  $\mu\text{g}/\text{ml}$ ), LL37-AuNPs (30 $\mu\text{g}/\text{ml}$ ) and AuNPs (30 $\mu\text{g}/\text{ml}$ ).

Immediately after the treatment the test was performed following this protocol.

The cells were washed in PBS and detached from the wells with 1ml of Trypsin-EDTA each for 3min in the incubator then the action of the trypsin was neutralized with 3ml of medium. Each sample was centrifuged at 300xg for 5min, the aspirated supernatant and the pellet resuspended in 200µl of PBS. A second centrifuge to remove the debris, 5min at 300xg, and then the PBS is eliminated. We are ready to fix the cells with 200µl of 4% PFA (paraformaldehyde) for 10min at room temperature. At this point we proceed with a half-wash by adding 500µl of PBS, centrifugation for 5min at 300xg to remove the PFA. Another wash, 400µl of PBS and centrifugation for 5min at 300xg, to eliminate excess PFA.

In order to facilitate the interaction of the antibodies with the receptor we proceed with the permeabilization of the membrane incubating the samples 30min with 90% methanol at room temperature. We complete the passage with the half-wash (500µl of PBS and centrifuge) followed by complete washing (400µl of PBS and centrifuge) to eliminate excess methanol.

Now the cells are suspended, fixed and permeable but before proceeding with immunocytochemistry we must prevent the formation of nonspecific bonds. In fact, we want the primary antibody to bind to the antigen, in our case EGFR; the problem is that the secondary antibody can attach anywhere. This artifact is avoided by using a blocking agent that occupies non-specific sites, in general a mix of proteins is used, specifically we have used a bovine serum. Once detached, centrifuged and fixed, the cells are suspended in 1% BSA (Bovine Serum Albumin) that is the solution used as a blocking. We divide each sample into two parts, one with primary antibody (dilution 1:20, 30min) and one without. The secondary antibody (dilution 1:2000, 30min) is added in all the samples.

Flow cytometers consist of a fluidic system, an optical system and an electronic system. In the flow cytometry technique, the suspension thus created is aspirated and passed through a nozzle so narrow as to ideally create a single cell flow.

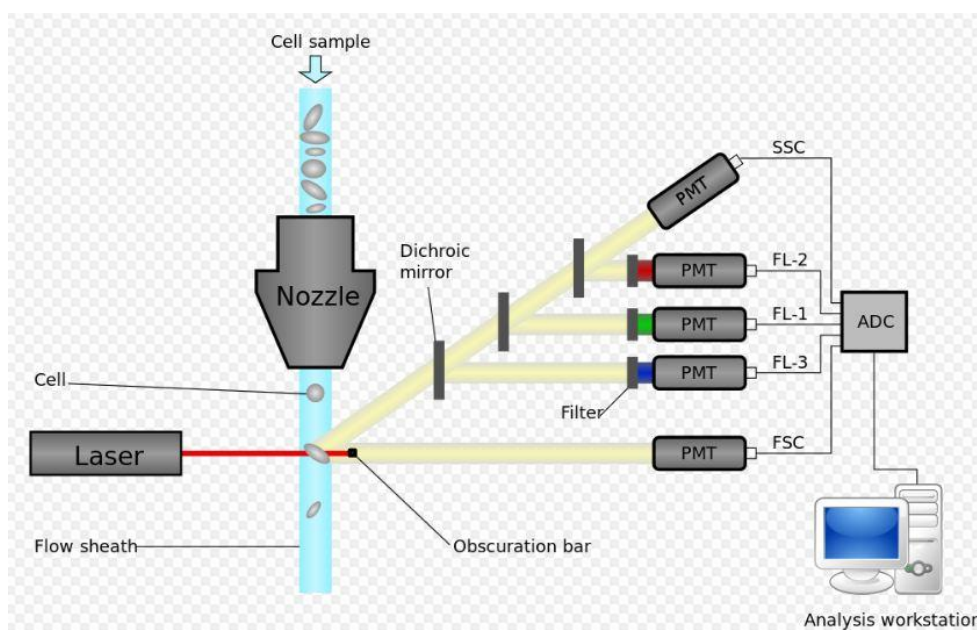


Figure 11-Schematic diagram of a flow cytometer [67]

There is a laser beam perpendicular to the flow. When this is crossed by the falling cell, it is interrupted. This is detected as an event. The size of the cells or particles / debris present in the suspension are determined according to how the light is scattered. If the cells have fluorescent molecules inside, they will absorb a certain wavelength. In our case, we used a small organic molecule (Alexa Fluor 488) stable, resistant to photobleaching and easy enough to combine with antibodies. The technology has higher potential, we can detect about seventeen fluorophores at the same time. Thanks to band-pass filters, only events confined within a small window of a specific wavelength of light are detected. The signals are converted into electronic signals and then analysed. The detector can calculate the intensity of the residual spectrum and therefore we can qualitatively calculate the amount of antibody. We can distinguish debris and aggregates from the single cell population (gating) [54]. Selecting this population, the software only counts the events that fall within the standard one. One of the most common problems, which we have also detected, is the autofluorescence of cells. The discriminant between one event and another is a threshold that we set to exclude unlabelled cells from counting.

A second problem often detected is the non-specific binding of the secondary antibody, to eliminate this artifact a control is prepared for each condition without primary antibody. Ideally if there is no primary presence, the secondary should not be detected as the whole sample has been subjected to blocking with bovine serum (1% BSA) but this occurs and it must be considered.

Therefore, considering the size, we choose the population; considering the artifacts of autofluorescence and non-specific bonds we choose the threshold. At this point we test all the samples and the software returns the percentages beyond the threshold. For each condition, 10000 events were considered. In the case under examination, only the cells expressed the receptor so it was decided to rely on another parameter output from the flow cytometry which is the Mean Fluorescence Intensity.

#### **4.4 Cell differentiation**

The potency of mesenchymal stem cells, i.e. the ability to differentiate into different lineages, makes them highly attractive for tissue / regenerative engineering and for clinical applications. Stem cell differentiation is dictated by a number of environmental factors that have not been fully discovered to date. Molecules such as LL37 [29] , [27] or even inorganic materials, such as Au NPs [42], [40], have already been shown to positively affect the differentiation of MSCs. In this work we try to understand if the nanoparticle formulation containing LL37 can increase the ostioinductive effect through two different tests: ALP (Alkaline Phosphatase) test , after 7 days ,and mineralization test through Alizarin-Red Staining, after 21 days [9], [10], [11], [44], [2], [27]. The differentiation of SCAPs showed the ability of these cells to migrate. In the circular wells, the cells from the first post-seeding moment tend to remain compact, they multiply occupying all the available space and then start (about the 10th day) an inward migration. We have documented this phenomenon through acquisitions of images under the microscope: the complete detachment of the monolayer from the walls occurred on about the 12th day then the monolayer began to fold back on itself until it then became a spheroidal structure. The cells created by the organized three-dimensional structures until they were trapped inside. This mechanism, sometimes very sudden, made it necessary to anticipate the mineralization test.

We have performed several experiments:

- Single administration of the treatment



- Administration of the treatment every 48h, during the change of the culture medium
- Limited time single administration (4h) with poor culture medium (1% Pen / Strep in KO-DMAM)

The culture setting has remained constant. At the same time, the 24-multiwell plates were seeded for ALP and Alizarin-Red Staining, each condition in the odontogenic medium was compared with the relative culture in maintaining media. After the usual 24 hours of waiting for complete adhesion, the treatment was carried out in the maintaining media; the culture medium with eventual peptide / NPs supplements was changed every 48h. The experiment was considered started from the first administration. The conditions, duplicated for the use of the two vehicles, are:

- LL37-AuNPs at concentrations of 30  $\mu\text{g}/\text{ml}$  and 60  $\mu\text{g}/\text{ml}$
- AuNPs at concentrations of 30  $\mu\text{g}/\text{ml}$  and 60  $\mu\text{g}/\text{ml}$
- LL37-peptide at concentrations of 8  $\mu\text{g}/\text{ml}$  and 20  $\mu\text{g}/\text{ml}$  which mimic the quantities of peptide present in the samples treated with LL37-AuNPs
- untreated cells

Each condition was tested in triple samples.

#### 4.4.1 ALP test

Alkaline phosphatase is an enzyme from the hydrolase family that catalyzes the removal of phosphate groups. It is found in many tissues but is overexpressed in case of bone growth or remodeling following fractures. Its role is therefore closely related to bone mineralization and is observed already in the first week in cell cultures in vitro [11]. On the seventh day both induced and non-induced cultures were evaluated.

To detect and quantify the presence of ALP in cells, an ELISA-based colorimetric test with absorbance at 405nm called 1-Step PNPP (p-nitrophenyl phosphate disodium salt, Thermo Scientific) was chosen. The reagent is stored at 4°C and must be equilibrated to room temperature for about 30min. The culture medium was aspirated, the possible residue was removed with a rinse of PBS (100 $\mu\text{l}$  / well). The PNPP 1-Step reagent is gently mixed end over end and added to the culture (200 $\mu\text{l}$  / well). Gently shake the multiwell at the end to be sure that the reagent is homogeneously dispersed in the well. For the correct and complete reaction the multiwell was incubated for 1h in an incubator at 37

° C. At the end of the 60min incubation the reaction was stopped, out of the hood, with 100µl per well of 2N NaOH (sodium hydroxide). As usual the multiwell was gently shaken. The reaction between enzyme and substrate generates a yellow color, the more intense the more the enzyme is present. At this point, it is already possible to see the difference between the dispersion of ALP in different conditions, but to quantify the staining, just transport 200µl from each well in a transparent 96-wellplate and calculate the absorbance at 405nm. A spectrophotometer and Gen5 software were used for the detection and presentation of the values.

#### **4.4.2 Alizarin-Red Staining**

Alizarin-Red is able to color the calcium deposits inside the tissues and cellular formations, in binding to calcium it precipitates and generates a color between red and orange. In fully mature tissues, the calcified nuclei become almost brown in color. The timing of formation of the calcified deposits were initially chosen on the basis of notions of literature, most of the authors referred to the 21st day of culture, and then they were adapted to the differentiation status of the monolayers obtained by us. A good compromise was found between 16 and 19 days. The protocol foresees three rinsing steps in PBS before fixing the cells in 10% V / V formaldehyde (in milli-Q water) for 15min. Once the fixative solution has been removed, the excess must be removed by performing three more rinses but this time in milli-Q water. These steps must always be done with great care to avoid damage to the monolayer. At this point everything is ready for staining, 500µl of Alizarin-Red solution (40mM, pH = 4.1) were used for each well of the 24-multiwell plate. Incubation lasts 20 min at room temperature under the action of a mild shaking. Once the excess dye has been removed, another 3 washes in milli-Q water lasting 5 minutes each. The very last step is necessary for storage, the monolayer would tend to dry out and is therefore preserved with 1ml / well of milli-Q water. To show the results the multiwells were scanned, each well was also photographed through a camera-microscope system (10X magnification).

Three methods of quantifying the state of mineralization have been tried but not with good results.

- A first method involves the use of 10% w/V cetylpyridinium chloride (CPC) in 10mM sodium phosphate (pH=7) [27], [42] [11], [44]. 100µl of this solution are used to cover the colored monolayer, 30min at room temperature on an orbital shaker. The solution is not very stable, it needs to be freshly prepared (1g of CPC in 10ml of 10mM sodium phosphate (pH = 7, 37 ° C)) and at 37 ° C to increase solubility and avoid precipitates. Probably the amount of reagent used was too small, the method proved to be unsuccessful as the readings at 570nm of the supernatant were not congruent with those clearly evident with the naked eye. Exposure times to the reagent were also increased up to 24h but no evident improvements were found.
- A second approach sees the use of 10% V / V acetic acid [10] to weaken the attachment of the monolayer (400µl per well), of cell scrapers to detach it completely and transfer it to a 1.5ml microcentrifuge tube. The samples are then vortexed for 30sec, hermetically sealed and inserted in a water bath at 85 ° C for 10min. The temperature is quickly lowered on ice (5min) and centrifuged for 15min at 20000xg. The supernatant is neutralized with 10% ammonium hydroxide, the pH must fall in a range between 4.1 and 4.5, and is now ready to be analyzed thanks to a spectroscope (OD405). The quantification is given by a calibration straight previously made by standards at different concentrations of Alizarin Red Solution. The problems with this technique lie in the high manual variability, some samples flake off during the procedure and others do not, with the result that the former are here inly more colored than the others. Furthermore, it is based on the assumption that the samples are in a truly prohibitive pH range.
- The third method is the one that comes closest to a realistic quantification. Since the acquisition of the images by scanner, ImageJ software has been used to analyze how much red there was in each well. At first, we set an equal threshold for all wells and calculated how many pixels exceeded this threshold by assigning a positive value. This was tested on a color image, in black and white and on a single channel in red. Another option was to calculate the darkness of the images. In each image of the bottom of a well

the brilliance of a rectangular or circular pre-posted area taken four times randomly was calculated. These values were complemented to one to obtain the darkness, then they were averaged and reported as a percentage of the area. Even this method of quantification, although remaining the fastest and most consistent, has not been adopted. The problems in this case are given by the image acquisition system. In scanners as well as in photos we find shadows and reflections probably given by the plastic of the multiwells.

## Results

### 1. Antimicrobial test

The antimicrobial activity of the LL37-AuNPs (60  $\mu\text{g/ml}$ ) was tested, with and without the use of the green laser, against different strains of bacteria through the combination of broth microdilution test and plate counting method. Several conditions are tested. The variables involved are many. The different bactericidal potentials between the free peptide and the peptide functionalized nanoparticles have already been tested in the previous works [48]. These studies showed that the antimicrobial activity of LL37-AuNPs is higher than the free peptide and bare AuNPs had no antimicrobial effect. In this work we explored to understand if the addition of a laser exposure (532nm, 0.5W/cm<sup>2</sup>) could further increase the formulation's antimicrobial activity, which could damage the bacteria membrane. With the introduction of the green laser, it is necessary to ask whether it could alter the bacterial growth as well as the surface plasmonic effect given by the combination of the laser and AuNPs.

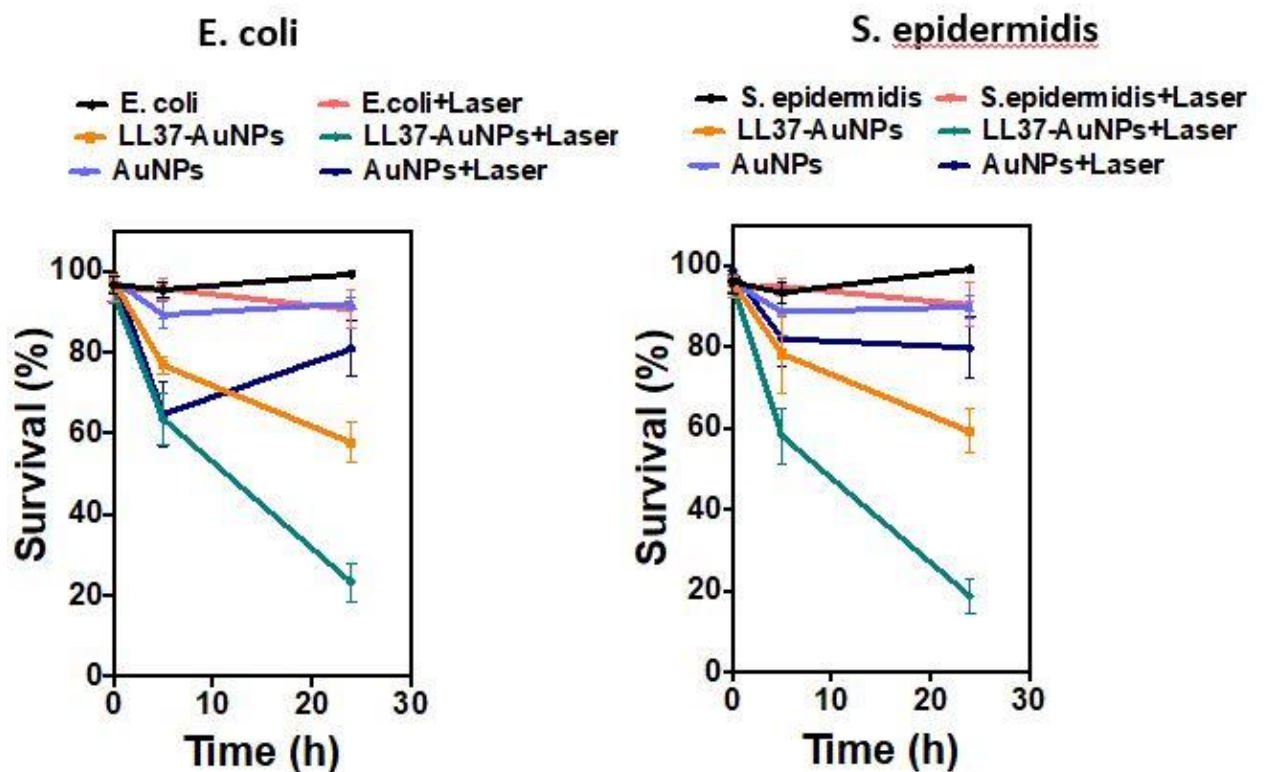


Figure 12a-Antimicrobial test of LL37-Au NPs (60  $\mu\text{g/mL}$ ) and Au NPs (60  $\mu\text{g/mL}$ ) in 10% human serum.

Here are the test results in 10% HS compared to four different bacterial strains *E. coli*, *S. aureus*, *S. epidermidis* and *E. faecalis*. The results are reported in percentage of survival

normalized to the value of the untreated bacterial culture. Aliquots from different treatment were withdrawn at time points (0h, 5h and 24h), diluted 100 times and plated on suitbale agar plates. The data in graph are average  $\pm$  standard deviation.

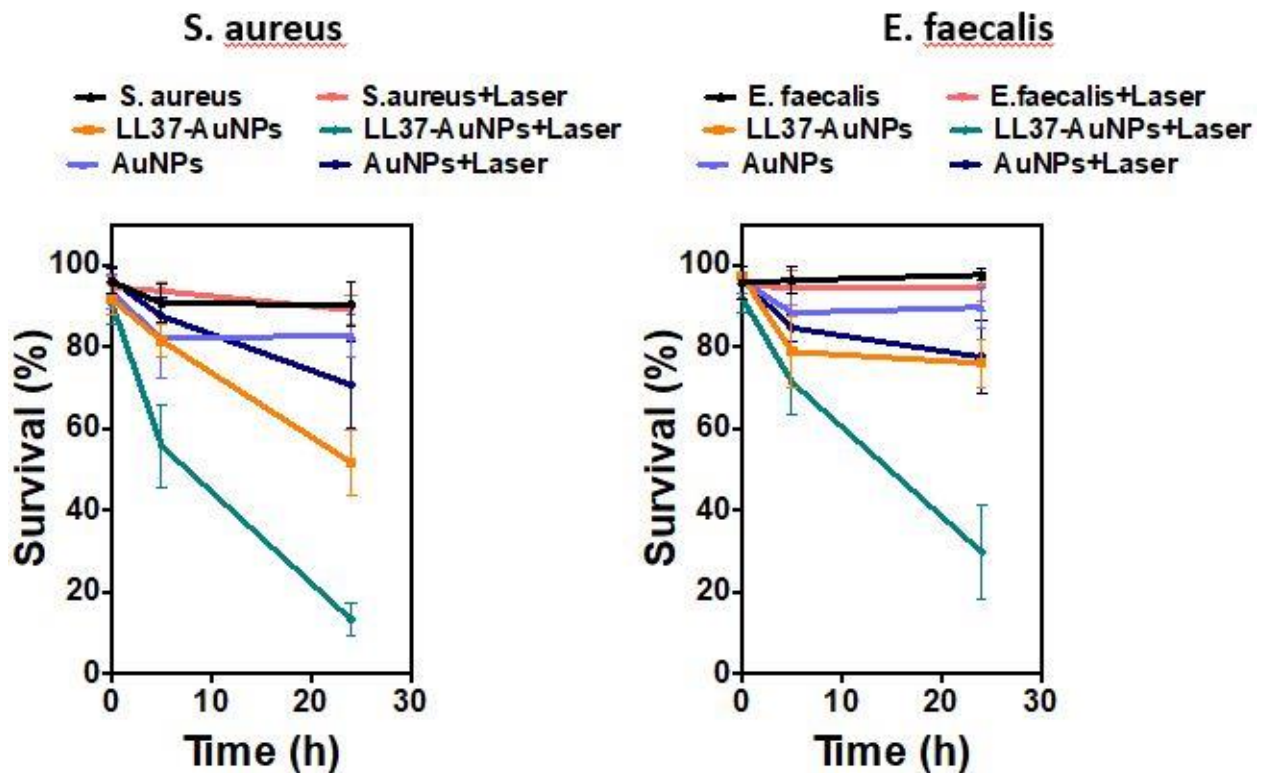


Figure 12b-Antimicrobial test of LL37-Au NPs (60  $\mu\text{g}/\text{mL}$ ) and Au NPs (60  $\mu\text{g}/\text{mL}$ ) in 10% human serum.

The green laser in the conditions of use (0.5W for 1 min on and 10 sec off for a cycle of three exposures) does not affect bacterial growth (*E.coli* and *S. epidermidis*) except for a minimum decrease of 10% compared to the untreated control after 24h of culture (figure 12a).

AuNPs in 60  $\mu\text{g}/\text{ml}$  concentration have no antimicrobial activity. The effect of the laser on AuNPs is highly strain-dependent; in some cases, it was very effective in killing bacteria in the first few hours. At 24h survival is in the range between 70 and 80%. These results indicate that there could be bacteriostatic effects that simply slow down the growth of the colonies, on some strains (e.g. *E. coli*) it is more evident than the others.

Analyzing the results of antimicrobial tests, it is immediately evident that the LL37-AuNPs in combination with the green laser have potent antimicrobial activity. Even if compared to the condition in which LL37-AuNPs have not been subjected to laser, there is a noticeable decrease in survival over time. The trend suggests that, as in the case of AuNPs, the laser causes initial damage to the membranes and that the high density of the AMPs immobilized

on the AuNPs facilitated strong bactericidal action. It goes below the 30% survival threshold in all the strains analyzed. The most tenacious strain is *E. faecalis*, which in the absence of laser exposure remains almost indifferent to LL37-AuNPs and only 20% of mortality is found (figure 12b).

## 2. Permeabilization

The purpose of this work is to understand the antimicrobial mechanism (especially the permeability of inner and outer membrane) of LL37-AuNPs in combination with green laser. The antimicrobial activity of the LL37-AuNPs (60 µg/ml) was tested, with and without the use of the green laser, against *Escherichia coli ML-35p* (*E. coli ML-35p*) through the broth microdilution test (every 30 min for 24h). The dyes added in solution,

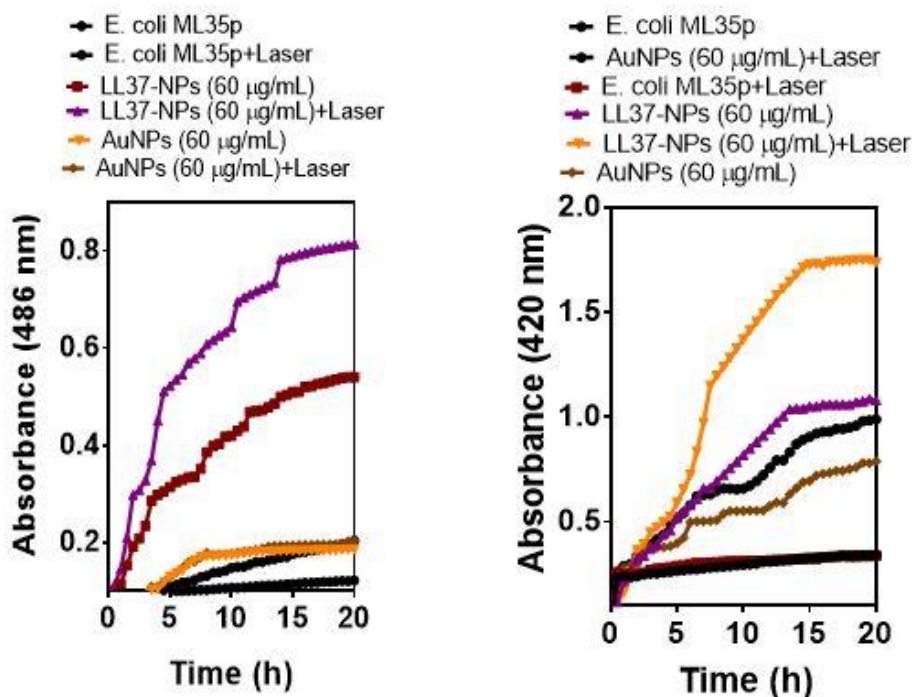


Figure 13-Permeabilization of the *E. coli ML-35p* membrane using NPs and laser. On the left the results for the external membrane (OM) on the right those for the internal membrane (IM).

react with transmembrane or cytoplasmic elements. Spectrophotometric reading is programmed with Gen5 software.

The results show that the LL37-AuNPs in combination with green laser condition is the best followed by LL37-AuNPs. With this condition the permeabilization of the external membrane occurs in a short time (5h), that of the internal membrane is a little more delayed (8h) but however very efficient (figure 13). The AuNPs, even if exposed to the laser, do not show significant outer and inner membrane permeability as compared to control.

### 3. Cell viability

In the literature, no reports were found which showed the odontoblast differentiation capability of LL37-peptide on SCAPs. Some studies, however, have tested the cytotoxicity of the free peptide on the closest relatives of the apical papilla cells, the DPSCs (Dental Pulp Stem Cells). In these studies, it is asserted that at concentrations equal to 5 and 10  $\mu\text{g}/\text{ml}$  LL37-peptide is not toxic, indeed it even increases the proliferation in the first days of culture [29]. In our experiments with bacteria, we used a quantity of LL37-NPs of 60 $\mu\text{g}/\text{ml}$  which contain approximately 20 $\mu\text{g}$  of peptide. We tested cytotoxicity effect of two different concentrations of nanoparticles: 60 $\mu\text{g}/\text{ml}$  (20 $\mu\text{g}/\text{ml}$  of peptide) and 30 $\mu\text{g}/\text{ml}$  (8 $\mu\text{g}/\text{ml}$  of peptide) against SCAPS. In addition to the control with untreated cells, we also tested cells treated with the same concentrations of PEG-coated AuNPs.

This test required the preparation of the calibration line. Starting from known standards we added the test solution (*CellTiter-Glo® Luminescent Cell Viability Assay*), measured the luminescence and calculated the straight line through the origin that best interpolated the points. The interpolation line was reliable ( $r^2 = 0.99$ ).

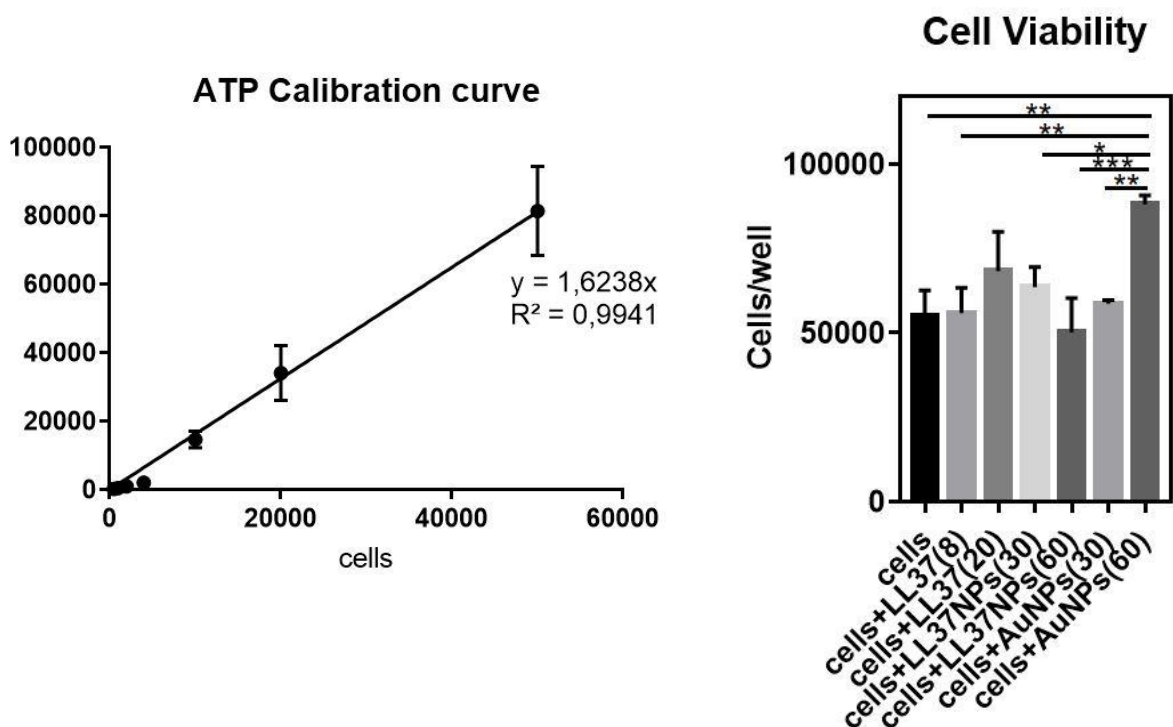


Figure 14-On the left calibration curve of CellTiter-Glo® Luminescent Cell Viability Assay with SCAPs. On the right, cell viability test results.



Three samples for each condition were analyzed, the graph (figure 14) shows the data relating to average and standard deviation. Cell viability is not affected by all conditions tested except where LL37-AuNPs are at a high concentration (60µg/ ml). This condition corresponds to the 20µg/ml concentration of peptide. The discrepancy between the two conditions can be explained, the peptide is internalized much more if it is immobilized than if it is free. Free peptide at high concentration and LL37-AuNPs at low concentration increase cell viability, albeit slightly. These differences are not statistically significant so these concentrations can be used in subsequent tests.

Finally, there is an increased viability of the cells treated with AuNPs (60µg/ ml), and therefore it required further research to understand the reason for enhanced cell viability.

#### 4. Cell proliferation

Seeding with lower cell density was useful, the cells did not reach confluence during the experiment, there was space for proliferation. Hoechst and PI were the two dyes that mark the DNA of the cells indicating live and dead cells respectively. Thanks to *IN Cell Analyzer 2200* and its software it was possible to calculate live and dead cells in different moments of culture, cell proliferation. The dyes did not prove cytotoxic even after a week and therefore it was preferred to refer to the same cell culture from the beginning to the end. In

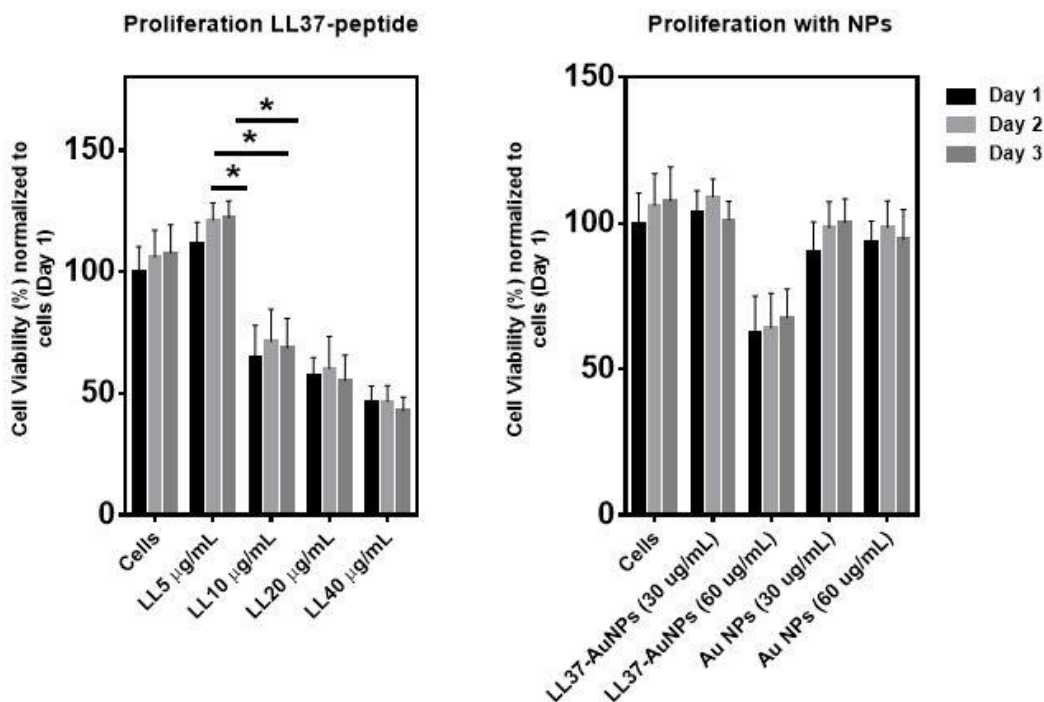


Figure 15-Percentage histogram for the cell proliferation test.

the figure, the condition of untreated cells on the first day was chosen as the percentage normalization term (100%). The data in figure is average  $\pm$  standard deviation (n=4).

This test showed that high concentration of free LL37 peptide and LL37-AuNPs induced cytotoxicity to SCAPs.

It must be remembered that the treatment used for this test deprives the cells of serum proteins for 4 hours. The culture medium used is without FBS, therefore the only stimulus is the LL37-peptide. Cells are much more sensitive to the presence of the peptide.

In fact, it can be seen (figure 15) how the number of cells decreases from the first day in conditions where the concentration of the peptide is 10  $\mu\text{g/ml}$  or greater. The same can be observed in higher concentration of LL37-AuNPs.

Instead, treatment with the lowest concentration of LL37-AuNPs (30  $\mu\text{g/ml}$ ) does not block cell proliferation, except slightly on the third day (figure 15). A proliferative slowdown could be an initial differentiating index. 30  $\mu\text{g/ml}$  of LL37-AuNPs corresponds to 8  $\mu\text{g/ml}$  of immobilized LL37 peptide.

We note, once again, that the formulation interacts better with the cells, it is able to expose the cells to a greater quantity of peptide without affecting the proliferation.

The negative control was cells treated with AuNPs. It does not deviate so much from trend of the untreated cells, as expected.

## 5. EGFR expression

The expression of EGFR analysis was carried out with flow cytometry, which shows that SCAPs express the EGF receptor and that LL37-NPs are able to increase this expression.

The direct interaction between the peptide and the stem cells of the apical papilla is confirmed. The results were analyzed and plotted using FlowJo software (v10 version). The first check carried out is that on cell autofluorescence and the blocking agent used (BSA). The cells have a certain autofluorescence also because the fluorophore used (Alexa Fluor 488) emits in

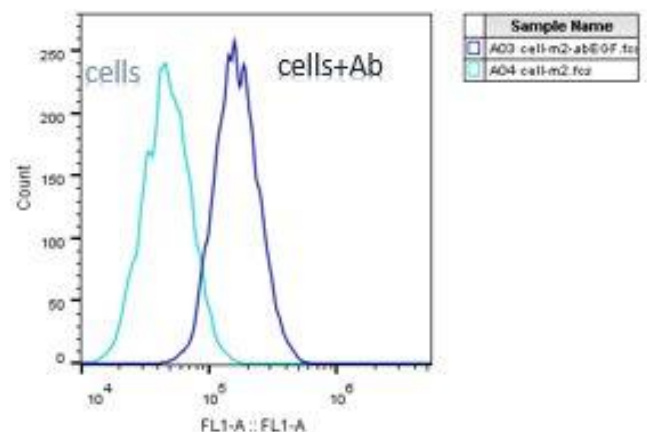


Figure 16-Graph showing the fluorescence of control cells and cells labelled with Alexa Fluor 488, used to choose the fluorescence threshold.

the band of the FITC channel which is the one most affected by autofluorescence. The effectiveness of the use of BSA as a blocking agent has been confirmed, cells not incubated with the primary antibody have a very low relative intensity. Similarly, the expression of the receptor was confirmed as the relative intensity of the marked ones is quite high. By comparing the two distributions (figure 16) of events just described, zero was set to obtain the percentages of expression of the receptor.

Some comparisons (figure 17) are reported to better understand the effect of free and immobilized peptide in the expression of EGFR. Although very little the cells treated with

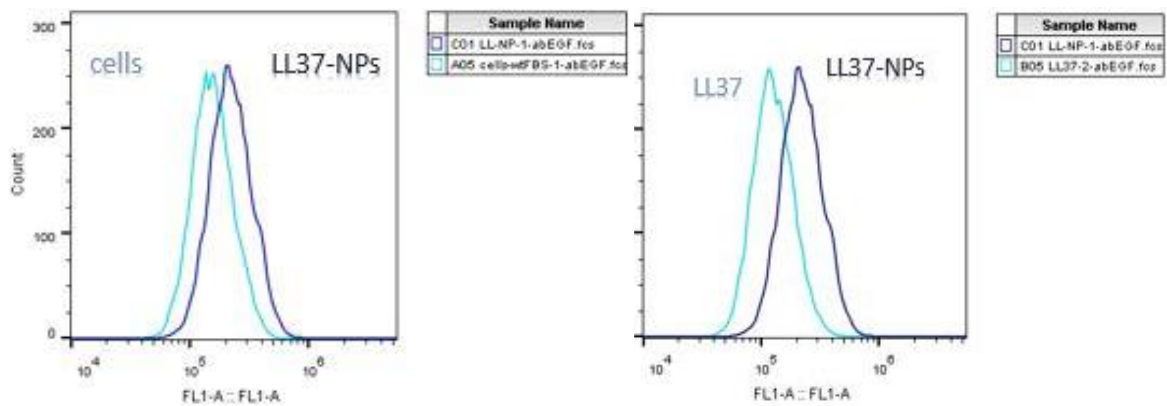


Figure 17-LL37-AuNPs treated cells compared with untreated cells (left) and free peptide treated cells (right).

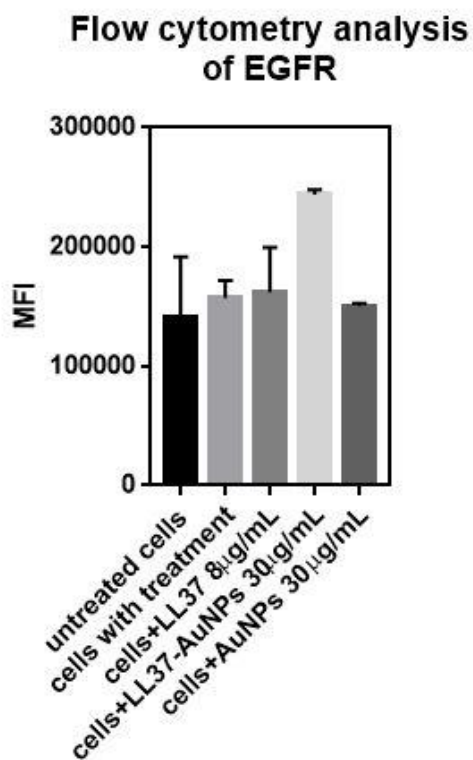


Figure 18-Mean Fluorescence Intensity histogram.

LL37-NPs showed higher percentages compared to the free peptide. For these reasons, another index known as Mean Fluorescence Intensity was analyzed. The values refer to the average and standard deviation calculated on the two samples per condition.

From the histogram shown here (figure 18), we can note that MFI is higher on average when using the LL37-AuNP formulation. Therefore, the expression level of the receptor was increased by the presence of LL37-AuNPs.

## 6. Cell differentiation

Differentiation tests were performed under three different administration conditions. The culture conditions were kept the same for all the experiments: cell density 10000 cells/well in 24-multiwell plate and change of medium every 3 days. Cell culture in both the basic and differentiation medium was tested each time. The NPs and peptides were added to the culture after 24h left to the cells to adhere to the bottom of the well.

Evidence of odontogenic potential is provided through two tests: ALP (at 7 days) and Alizarin Red Staining (between 15 and 21 days). The timing of the mineralization tests has been adapted to the folded state of the monolayer that has been observed.

These microscopic images show some examples of the phenomenon (figure 19).



*Figure 19-Microscopic images showing the folding of the cell monolayer. They refer to culture in differentiation medium after 10, 12 and 13 days respectively from left to right. The elongated shape of the migrating cells can be seen.*

In all experiments the data were normalized to the control of untreated cells (100%) and refer to the average and standard deviation calculated on three samples for each condition.

### 6.1 Single administration

The first experiment aimed to understand if effects on cell differentiation could have had with a single administration of the nanoformulation. At the first change of culture medium, after 3 days, the monolayer was rinsed with PBS to eliminate non-internalized NPs or peptides.

APL test (figure 20) showed that in the differentiation medium with LL37-AuNPs we have slightly higher values but there are no relevant differences.

In the maintaining culture medium, we have a sub-regulatory effect of AuNPs, contrary to what was expected. Here too, as in the cell viability test, can be an error.

The ALP test involves the use of a spectrophotometer with which the red color of the AuNPs could have interfered.

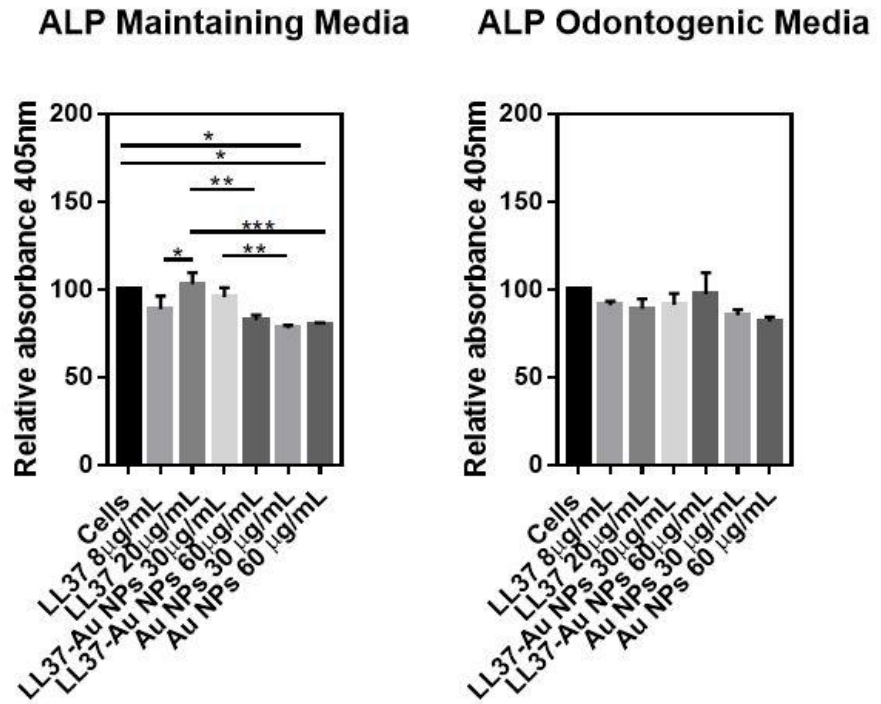


Figure 20-ALP test performed after 7 days of culture with single administration.

We considered the possibility that the effects could be found in the long-term, so we also performed the Alizarin Red Staining.

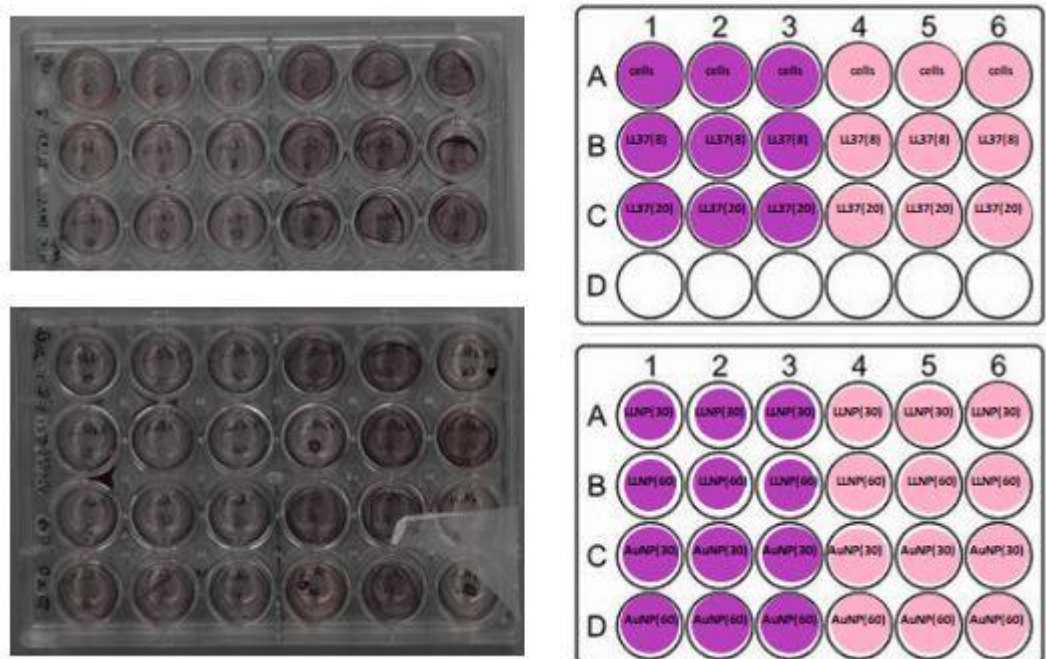


Figure 21-Alizarin Red Staining performed after 18 days of culture with single administration and an experimental setting scheme (on the right the samples grown with a differentiation medium). The images were acquired with a scanner.



From the images (figure 21) it is clear the difference between the cells grown with maintaining medium (on the left) and those grown with a differentiation medium (on the right). The wells treated with odontogenic culture medium have a much more intense color. This indicates that the dosages of the additives present in the odontogenic medium differentiate SCAPs to odontoblast like cells. However, it would seem that SCAPs are completely indifferent to LL37-peptide or LL37-AuNPs in these modes of administration. There are no appreciable differences between the various conditions.

Like the Alkaline Phosphatase test (figure 20), Alizarin Red Staining (figure 21) has also shown that this type of treatment is too bland. Anyway, the little evident results have pushed us towards more incisive administrations like the ones that follow.

## 6.2 Multiple dosing

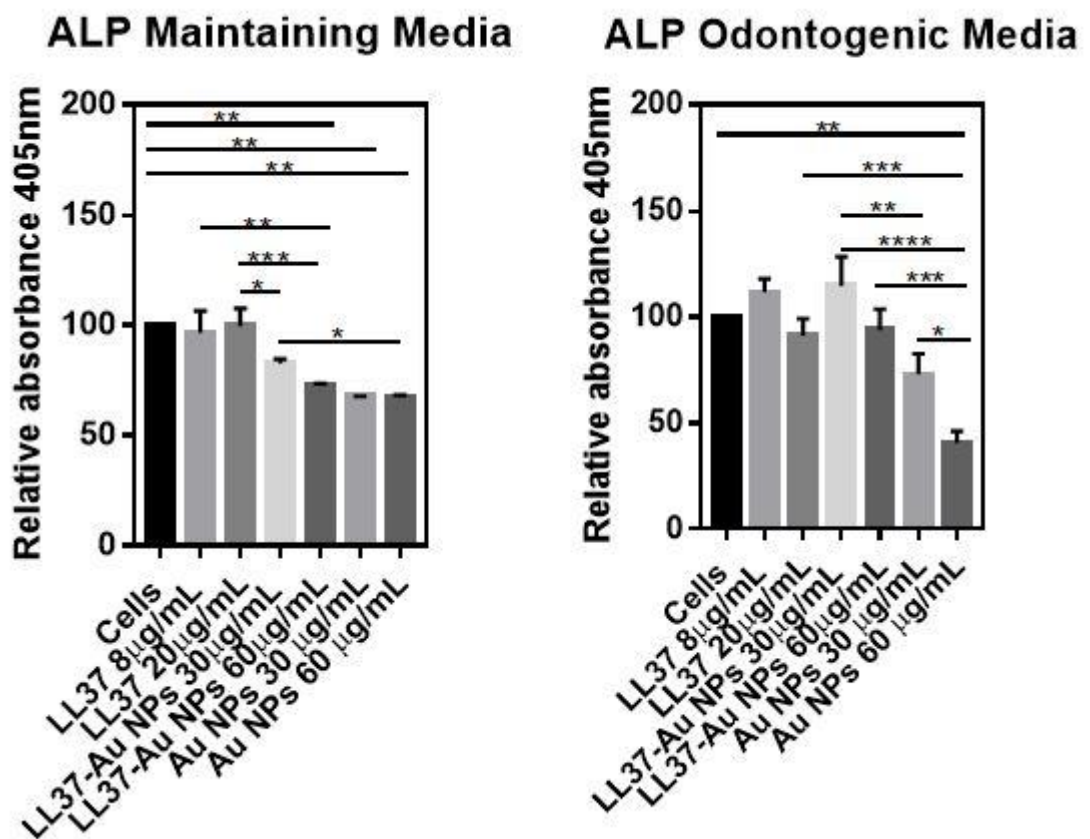


Figure 22-ALP test performed after 7 days of culture with multiple administration.

The risk of administering peptide and NPs every 48h is that the level of cytotoxicity is reached very quickly. On the other hand, assuming drug release applications,

prolonged contact with NPs is more realistic. In this experiment the administration was repeated with each change of the exhausted medium (i.e. every 3 days). In this case we get more promising results. The ALP test confirms that doses at low concentrations but repeated can increase the production of Alkaline Phosphatase (figure 22). Especially if we compare the results of the LL37-AuNPs with the AuNPs we see that the differences are consistent. It could be an error, in this case too, given by the interference between the instrument and the color of the AuNPs but the mineralization test clarifies any doubt.

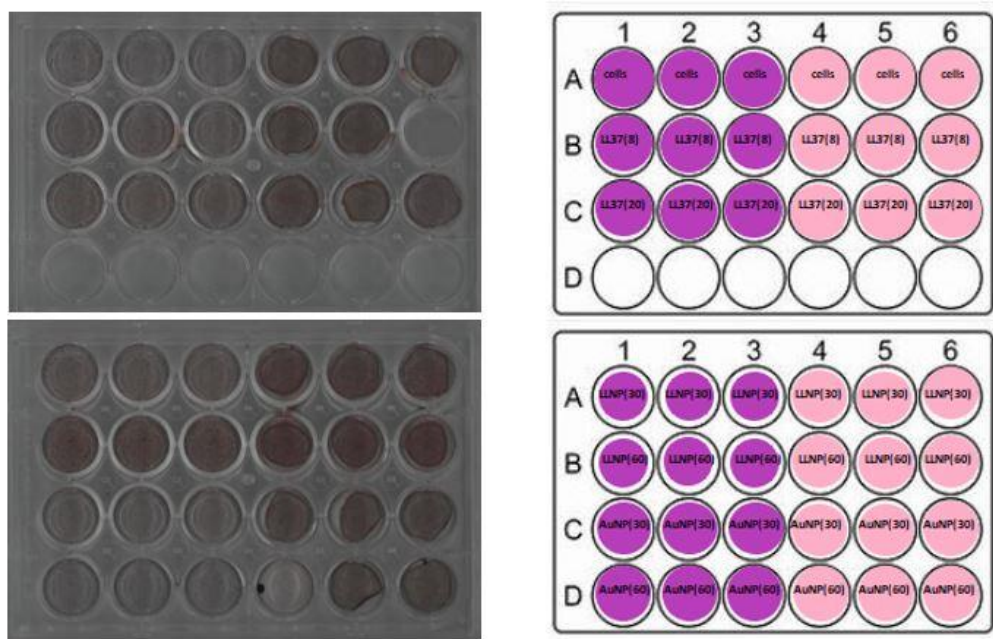


Figure 23-Alizarin Red Staining performed after 16 days of culture with multiple administration and an experimental setting scheme (on the right the samples grown with a differentiation medium). The images were acquired with a scanner.

As can be seen from the images (figure 23), there are many more calcium deposits in the wells treated with multiple doses of LL37-AuNPs. In this case we clearly distinguish the various conditions. Samples treated with LL37-AuNPs show a dose-dependent staining. Mineralization is more evident where the concentration is greater. This phenomenon is present not only in samples grown with osteogenic additives but also in the base culture medium. The treatment was successful.

### 6.3 Limited-time single administration with poor culture medium

The last treatment tested is aimed to understand if the presence of other signalling pathways could influence the differentiation of SCAPs. The cells were contacted with peptide and NPs for 4h in a poor culture medium (1% V/V Pen/Strep in KO-

DMEM). After the treatment, the whole culture environment was restored. From proliferation tests (figure 15) we have understood the high sensitivity of cells to this type of treatment. Although the best results have been achieved in multiple dosing case, it was decided not to repeat the treatment.

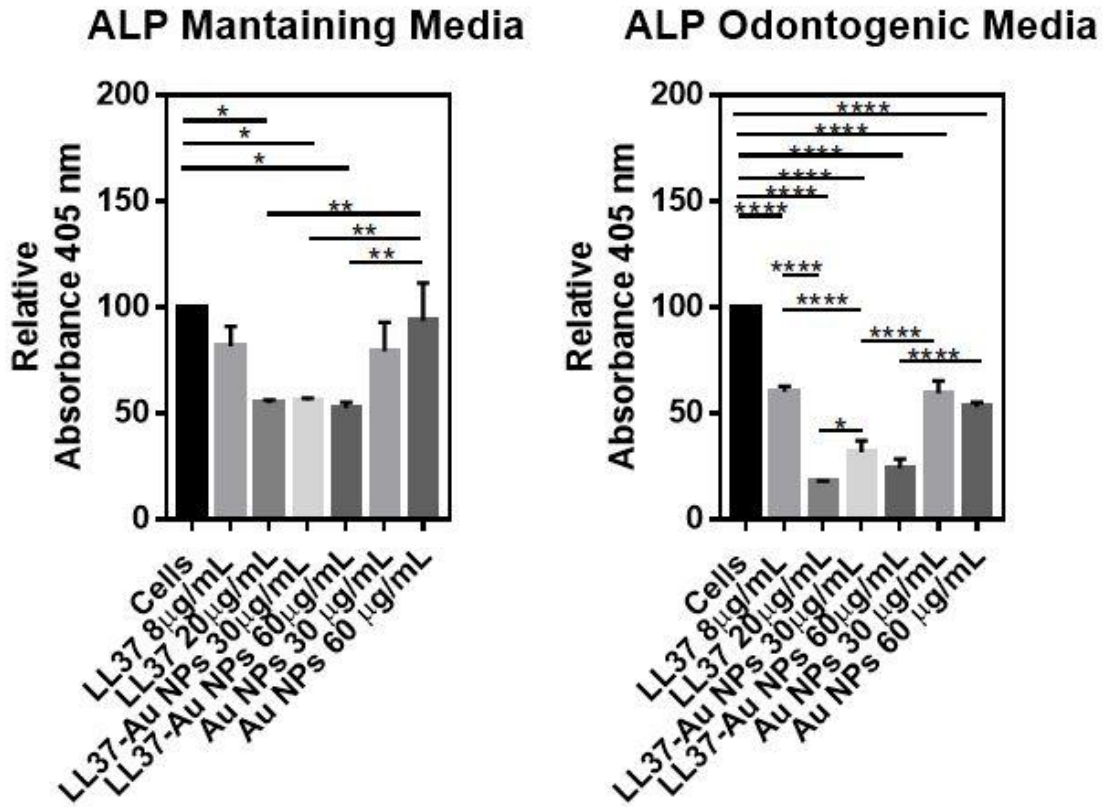


Figure 24-ALP test performed after 7 days of culture with 4h single administration in 1% V/V Pen/Strep in KO-DMEM.

The results of the ALP test are probably affected by the cytotoxicity of the nutrient-free treatment. We observe, in fact, a halved expression of Alkaline Phosphatase in many of the conditions (figure 24).

This would suggest that treatment does not benefit odontogenic differentiation. Actually, the test is usually normalized to the protein content or the number of cells present in the well. Looking at the microscope images (figure 25, 26, 27) and

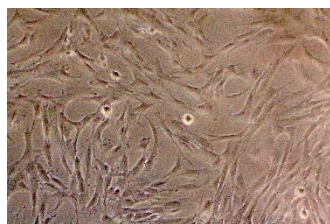


Figure 25-Cells 48h after treatment with poor culture medium.



Figure 26- Cells 48h after treatment with poor culture medium and AuNPs (60µg/ml).

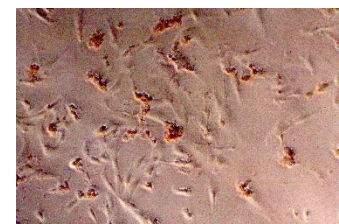
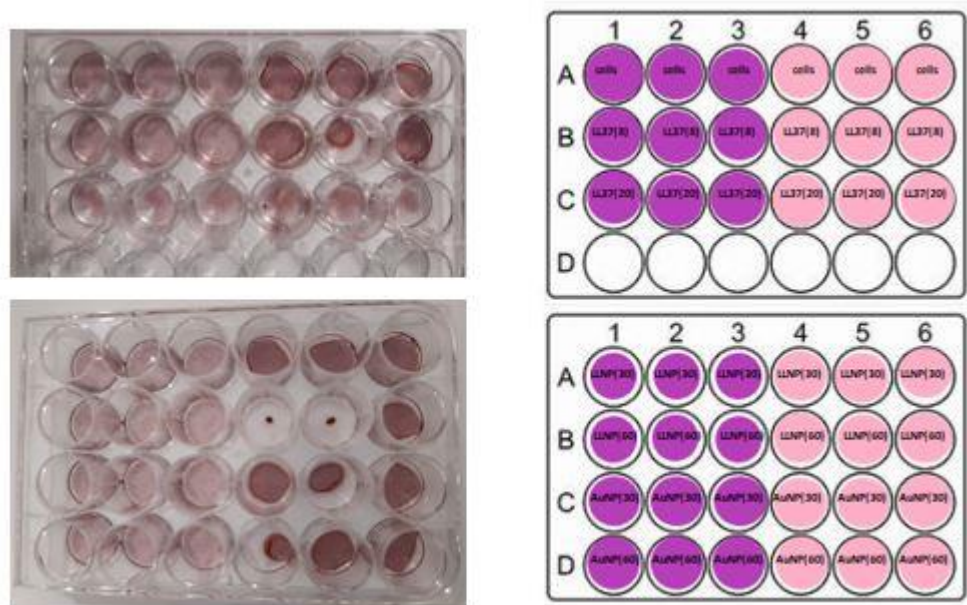


Figure 27-Cells 48h after treatment with poor culture medium and LL37-AuNPs (60µg/ml).



considering the results of the cell proliferation test (figure 15), it is clear that the problem lies in the cytotoxicity of the FBS-free medium. Free peptide and NPs with immobilized peptide, stress the cells. This, added to the poor culture medium, makes the graph untrue.



*Figure 28-Alizarin Red Staining performed after 18 days of culture with 4h single administration in 1% V/V Pen/Strep in KO-DMEM and an experimental setting scheme (on the right the samples grown with a differentiation medium). The images were acquired with a camera.*

The mineralization test confirmed that a single administration is ineffective to induce differentiation. We do not distinguish the conditions, except for the samples treated with 20 $\mu$ g/ml of LL37-peptide where, clearly, the monolayer has never been created (figure 28). This condition is unsustainable for cells that almost completely stop their growth and, therefore, are not even able to differentiate.

## Scaffolds in regenerative endodontics

In regenerative endodontics many studies are aimed at the use of scaffold. The currently recommended technique is revised because *apexification* supports apical closure but does not promote root ripening. In nature, the blood clot (cross-linked fibrin) created after trauma acts as a scaffold. Thanks to the endogenous growth factors, the SCAPs are populated that populate the scaffold and start the tooth regeneration (*evoked bleeding (EB)*). However, the usual decontaminations, using intracanal medicaments, tend to weaken the stem cells and affect the regenerative process. A strong need therefore arises to combine antimicrobial factors and scaffolding that can encourage tissue regeneration. In the literature various techniques are proposed to realize scaffolds. Gas foaming and salt leaching techniques have been proposed to obtain microporous scaffolds. The possibility of using nanofibrous scaffolds has also been investigated. For example, the molecular self-assembly allows to inject the substance on site and generate a gel through non-covalent interactions. In addition to insufficient mechanical properties, with this approach it is very complex to control the size/shape of the pores. Although it cannot be injected, electrospinning allows greater control of the structure, the possibility of varying geometries and compositions. A tubular structure has also been proposed to facilitate the closure of the apex and the thickening of the dentine walls. Another proposed technique is thermally-induced phase separation (TIPS), a component is thermally eliminated leaving pores. Research is very active in this field. Over time, various techniques, materials, supplementary agents (cells, growth factors and antimicrobial agents) have been proposed but the optimal solution is still being sought [55] [56] [57].

### 1 Gelatin-LL37-AuNPs nanofibrous scaffold

For in vivo applications, it would be convenient to obtain the treatment described in the previous chapters in a form more similar to a human tissue as well as easily applicable and transportable. In vitro the experiments were carried out in suspension, in vivo we need a scaffold to support the LL37-AuNPs. From these needs came the idea of developing a biocompatible and biodegradable matrix capable of offering a large surface on which to incorporate the NPs. The antimicrobial agent would be necessary in any application as the large exposed surface is an perfect environment not only for the host cells but also for the bacteria [58]. In the first period, the scaffold acts as a three-dimensional support in the growth of a tissue, replacing the extracellular matrix. At a later time, its ability to degrade in a physiological environment makes complete tissue reconstruction possible. The idea is to support cell growth until it is needed and

then dissolve and leave no trace of foreign intervention. Tissue engineering is concerned with combining scaffolding, cells and signaling molecules. To optimize the integration in vivo we try to imitate the topography, architecture and composition of human tissues. Mechanical signaling is also not to be underestimated. A certain state of tension can affect cell differentiation. The insertion of NPs increases the mechanical properties of the structure.

In the case under consideration, we thought of a planar nanofibrous support with random orientation. The choice of technique fell on one of the most studied devices in this field, namely electrospinning. This technique allows us to create planar three-dimensional structures and to cover any implant objects. Electrospinning is a production technique that allows to obtain continuous filaments with a controlled diameter from polymer solutions. The technique works if the solution has a concentration higher than the entanglement concentration ( $C_e$ ) [58].

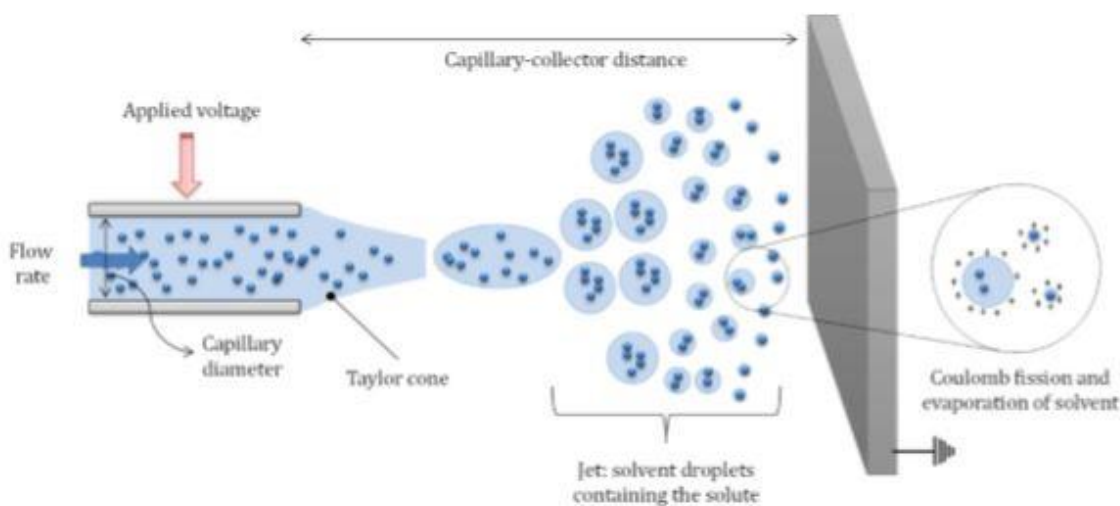


Figure 29-Diagram of the electrospinning process [58].

The stretching of the polymeric material is caused by an external electric field between the capillary and the collector which accelerates the charges present in the solution. The so-called Taylor cone is generated, the droplet at the tip of the needle takes on a conical shape until the electrostatic forces prevail over the surface tension of the fluid and then starts to spin. During the flight between the syringe and the collector the solvent evaporates and, in the case under examination, this makes cross-linking possible [59]. Using a flat collector, we obtain a random deposition of the nanofibers.

The nanofibrous structure offers a very high exposed surface, in this way we increase the ability to interact with the nanoparticles and that of the NPs with the cells. This type of structure also offers a high porosity and interconnectivity necessary for migration, cellular organization,

improved nutritional intake and, at a later time, for tissue vascularization. Every aspect of the technique, from the diameter of the fibers to their arrangement, can affect the cells (i.e. proliferation, morphology, phenotype).

The material to be used must be biocompatible and biodegradable in a relatively short time. Degradation must have a rate compatible with tissue growth. In this case, we have chosen to use a natural material of animal origin (biopolymers), the gelatin. Synthetic materials are less problematic on a practical level but are more difficult to integrate with the tissue. Natural materials promote cell adhesion by providing adequate chemical signals (bioactivity) and causes a low inflammatory effect. However, with natural materials it is not possible to use high temperatures, solvents and aggressive working conditions [58], [59]. They are more delicate and for this reason they are modified adapting them to the technique.

Gelatin is composed of polypeptides (abundant in glycine, proline and hydroxyproline) and is derived from the partial hydrolysis of collagen, an adhesive protein. It is commonly used because it is very similar to collagen but costs significantly less. Gelatin exhibits ligands (e.g. RGD sequence) that promote cell attachment and target sites for cellular metalloproteinases (MPP) that allow for the in vivo biodegradation [60].

In literature it is possible to find examples of gelatin electrospun with organic solvents or acids. There is the risk that solvent traces, that have not evaporated in flight, may remain trapped in the fibres. They can come in contact with the cells for which they are toxic. In any case, for biomedical applications we need a certain stability in an aqueous environment, the gelatin is water soluble which makes it necessary to crosslink. Cross-linking allows you to create stable transverse bonds between the polymer chains in order to avoid their dissolution. This treatment is usually performed downstream by aldehydes, carbodimides, enzymatically or physically (e.g. UV radiation exposure). The solution techniques suffer from problems of swelling in water while the physical ones have a low degree of crosslinking. The technique also requires a high fluidity of the material which therefore cannot be crosslinked before.

A study gave birth to an electrospun gelatin protocol starting from a non-toxic aqueous solution and cross-linked at the same time as the creation of the nanofibers. This is made possible by the study of the various parameters to be set on the instrument and by the phase transition of the sol-gel material at 50 ° C [59].

Type A gelatin (Sigma-Aldrich) was used. Gelatin is a collagen derivative, for medical applications it is manufactured according to two processes. Type A gelatin is produced from porcine skin with an acid treatment and type B gelatin is produced from bovine skin with a lime-based treatment.

The cross-linking agent GPTMS ( $\gamma$ -glycidoxypropyltrimethoxysilane) at the two ends has a group that binds gelatin and a group that binds other GPTMS molecules.

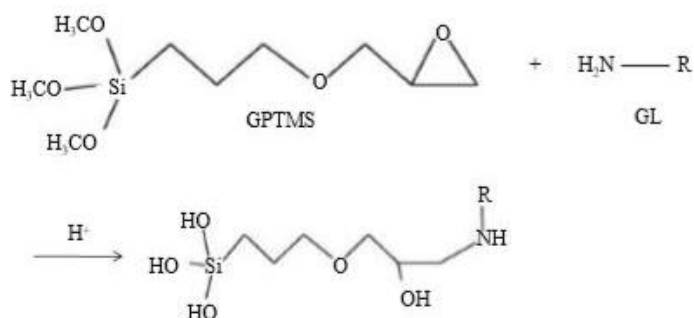


Figure 30- The equation represents the reaction between oxirane rings on the GPTMS and amino groups on the gelatin chains and the acid catalyzed hydrolysis that generates the pendant silanol groups (Si-OH). [59]

The oxirane rings react with the amino groups present in the gelatin chains while the trimethoxy groups, become pendant silanol groups (Si-OH) through hydrolysis, react with each other generating Si-O-Si bonds. Since the latter are the result of a condensation reaction, these bonds are more likely to form during the evaporation phase of the solvent.

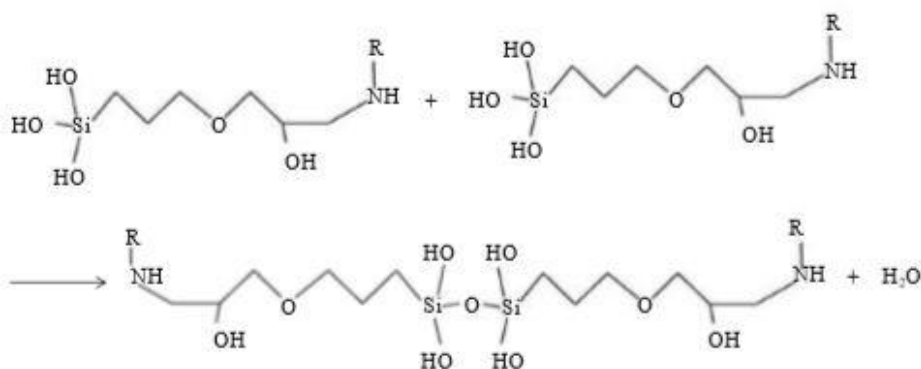


Figure 31-The equation represents the condensation between two silane groups, Si-O-Si bond is formed [59].

This mechanism allows to have an extrudable solution since, unlike other pre-process crosslinkers (e.g. genipine), it does not crosslink in solution.

## 2 Nanofibres preparation

The volumetric pump (KDS210 by KD Scientific), the collector and the electrode are mounted in a ventilated hood equipped with two electric lamps that maintain the temperature at 50°C

and a vapor extractor. The voltage generator (Glassman High Voltage PS / EL30R01.5-22) is placed outside the hood.

Gelatin nanofibres were made according to the described protocol [59]. An electrospinning with a single syringe pump, a 21 Gauge needle and a flat collector was used. A solution of Type A gelatin (GL) and water at 15% w/v is created. We prepare 5ml of this solution and mix it on a magnetic stirrer at a plate temperature of 50°C. After about 3 hours the solution is visibly homogeneous, and it is possible to proceed with the insertion of the cross-linking agent GPTMS. The (liquid) GPTMS must be added in relation to the amount of gelatin present in the solution, 92 µl for each gram of GL and react for 30min at 50°C. It is essential that, like the stirrer plate, the electrospinning chamber is also kept at a temperature high enough to avoid solidification of the GL. Before withdrawing the fluid, it is necessary to make sure that the hood temperature is optimal and that both the collector and the needle have been prepared. The collector is an aluminium foil fixed on a rectangular support; the needle must have an opening orthogonal to the flow. The potential difference is set at 30kV, the flow rate at 1.5 ml/h on the syringe pump and the needle tip is placed 12cm from the flat collector. We are ready to place the syringe, connect the cables and start.

The parameters described are the result of a careful study: the GL concentration (% w/v), the flow rate, the nozzle-collector distance and the intensity of the electric field have been optimized to obtain the narrowest dimensional distribution, the lowest concentrations of defects and the desired porosity.

With the help of tweezers, we can detach squares of nanofibrose matrix. We try to obtain all the membranes of the same area (2cm<sup>2</sup>) but the thickness remains very complex to be kept constant.

### **3 Conjugation**

The conjugation between electrospun nanofibers and NPs can occur in different ways. We have the possibility to insert the NPs in solution (we will obtain a random dispersion), to use them for an external coating (e.g. through sputtering, impregnation, electrospinning / electrospaying [58]) or we can trap them inside (coaxial electrospinning [58]). Depending on the conjugation and the arrangement, we will obtain different release kinetics. In the present case, we would like to achieve both a short- and long-term effect. In fact, the task of LL37-AuNPs is to eliminate bacterial infection but also to interact later with the stem cells recalled on the site.

Therefore, the ideal would be to have NPs both externally (fast release) and internally (slow release) [58].

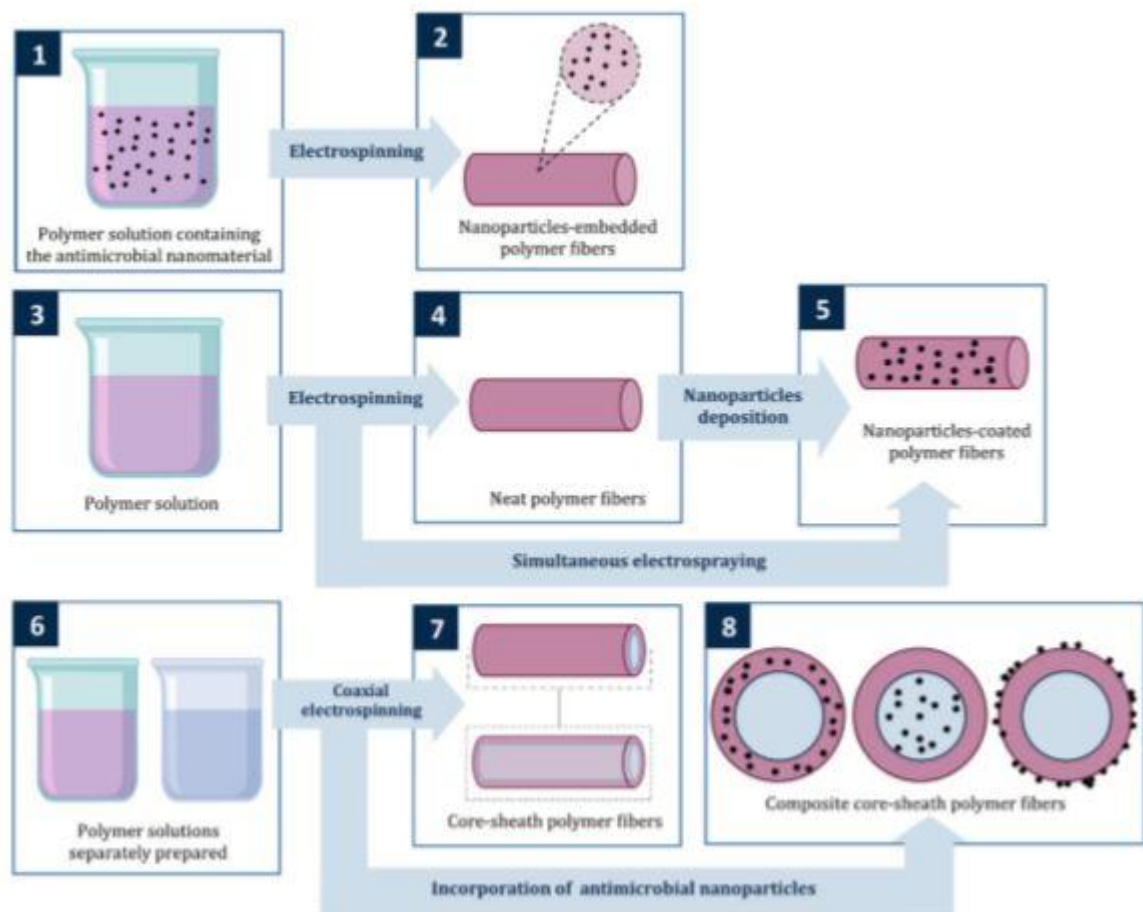


Figure 32-Different approaches to create composite fibrous materials engineered by electrospinning [58].

Various examples of scaffold loaded with antimicrobial nanoparticles are present in the literature (zinc oxide, titanium dioxide, silver and gold nanoparticles), among these the most studied are those loaded with AgNPs. For example, in one article a scaffold of gelatin loaded with AgNPs was studied and it was shown that, although the NPs are initially cytotoxic, the structure acts as a support for cell growth [61]. In another work, by combining antioxidants (cerium oxide nanoparticles (nanoceria, NC)) with GL electrospun nanofibers, a support for neuronal growth was created. The combination of topographical stimuli and NC favors the neuronal phenotype [62].

Initially it was thought to insert the LL37-AuNPs into the solution, as in the previous examples. This would have allowed to avoid the functionalization step and to obtain the release of part of the NPs delayed at the time of degradation/dissolution. The setting of the machine was not changed because the NPs seemed to almost stabilize the GL solution. The viscosity was slightly increased but still such as to be extrudable. The nanofibers thus created were

characterized morphologically by SEM without finding more manufacturing defects than the gelatin nanofibers. The release tests in water showed no leaching. By carrying out the first antimicrobial tests we realized that the quantity of LL37-NPs exposed was not enough, the degradation/release times (15 days) were not coincident with those of the tests (24h). In order to exhibit antimicrobial activity, LL37-AuNPs must be present on the surface of nanofibers [58]. Another factor could be the damage to the peptides subjected to the stress of spinning [58]. With these considerations, the gelatin fibers were made and subsequently functionalized with the NPs.

Two different conjugation approaches were tested to functionalize the surface of the fibrous membrane of gelatin with the LL37-Au NPs. One of the roads envisages the formation of covalent bonds exploiting the chemistry of carbodimides to activate the carboxyl groups of gelatin that react with the LL37 peptide. The other way is simpler, less expensive and is then found to be the most effective, it involves the formation of non-covalent bonds given by the electrostatic interaction between the amino groups of the GL and the gold bulk of the nanoparticles.

To activate the -COOH groups with EDC-NHS a solution of EDC (1mg) is created in PBS (1ml, PH = 7.2) and is added to 1mg of NHS (at room temperature). Stirring in a tube with the nanofibers these are deprotonized, after 15 minutes the reagents are removed. Before inserting the suspension of nanoparticles, wash in PBS and then in milli-Q water to avoid aggregation.

For the second method we don't need activation steps.

For both conjugations, 0.5ml of LL37-Au NPs suspension is incubated overnight with 2cm<sup>2</sup> nanofibres. The interaction with nanoparticles deriving from processes with different pH (5 and 7.5) was tested. To remove the excess, the membrane is washed in milli-Q water and dried. The conjugation is done but in order to use the samples these must be sterilized (30min each side under UV lamp). To maintain the original size and shape, the membranes must be dried on a flat surface; to accelerate the process a nitrogen jet dryer can be used.

#### **4 Antimicrobial tests**

Exactly as for nanoparticles, nanofibers have also been tested. The experiment foresees the following conditions:

- bacteria in contact with nanofibers functionalized with LL37-AuNPs irradiated with the laser
- bacteria in contact with nanofibers functionalized with LL37-AuNPs



- bacteria in contact with nanofibers functionalized with AuNPs irradiated with the laser
- bacteria in contact with nanofibers functionalized with AuNPs
- bacteria irradiated with the laser
- untreated bacteria

The broth microdilution method assisted with plate dispersion is still the most effective method for testing the antimicrobial action of the membrane. The swelling of the gelatin helps in this case to keep the membrane at the bottom of the tube, the membrane absorbs the culture liquid and does not float.

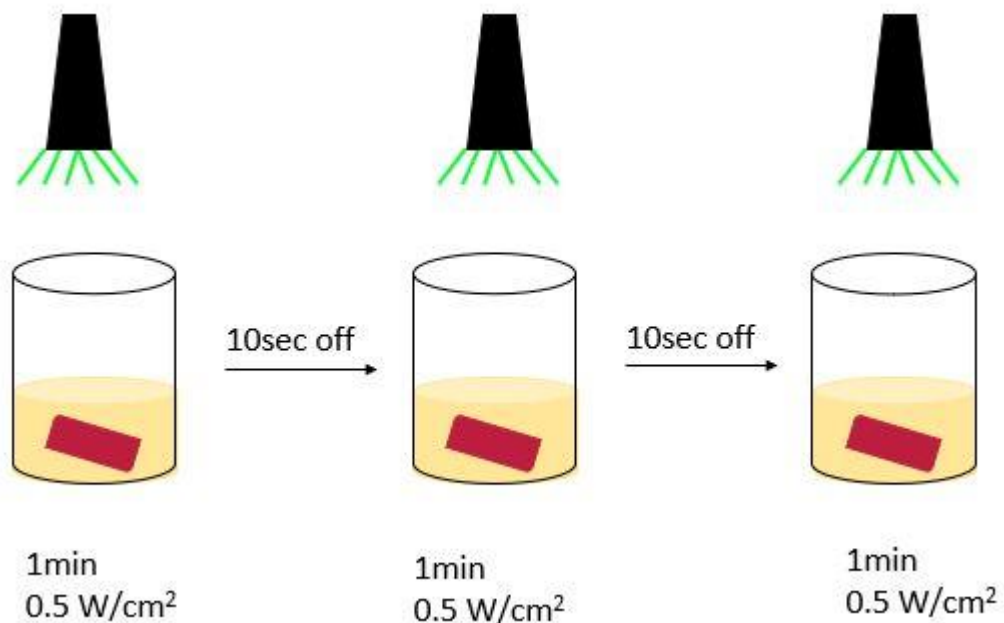


Figure 33-Procedure scheme for green laser exposition with fibers

Not knowing the quantity of nanoparticles deposited on the nanofibers, we always consider the same surface area ( $2\text{cm}^2$ ). As described above, the bacteria are grown, counted, diluted in PBS and re-cultivated the 10% V/V HS solution in contact with the nanofibers ( $10^5$  cfu / ml). Spreading on the agar dish is performed at 5h and 24h, and the count is always after 24h of culture in an incubator. Antimicrobiality has been tested against the same strains: *Escherichia coli* (*E. coli*), *Staphylococcus aureus* (*S. aureus*), *Enterococcus faecalis* (*E. faecalis*), *Staphylococcus epidermidis* (*S. epidermidis*).

As seen for NPs in suspension, laser exposure of bacteria alone is harmless. The action of LL37-AuNPs does not exceed 40% of mortality, as well as that of AuNPs with laser treatment.

The combination of LL37-AuNPs and laser treatment is the condition with the highest bactericidal potential.

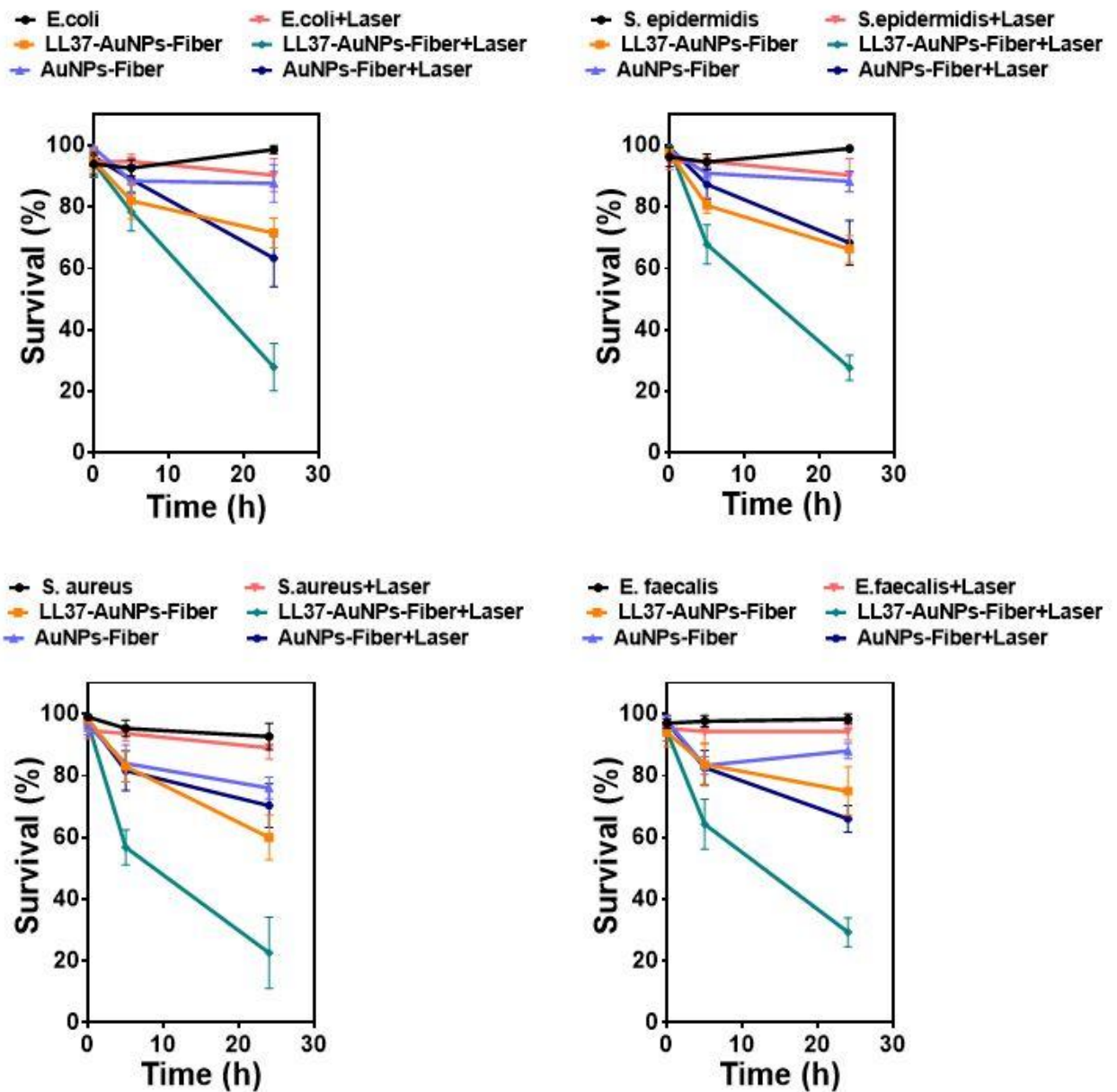


Figure 34- Antimicrobial test of LL37-Au NPs-Fibers and Au NPs Fibers in 10% human serum.

Gelatin fibers, being a natural polymer, act as nourishment for bacteria, so these results are better than expected. It reaches a mortality rate of 70-80% despite the gelatin. Probably the reasons are the high exposed surface, the high concentration of nanoparticles and their possibility of leaching.

The test to understand the antimicrobial mechanism once again uses the engineered strain *Escherichia coli* ML-35p (*E.coli* ML-35p), this time however it is not possible to read

continuously in the plate reader. The presence of the membranes would alter the results, it is necessary to proceed manually every hour to read the two dyes.

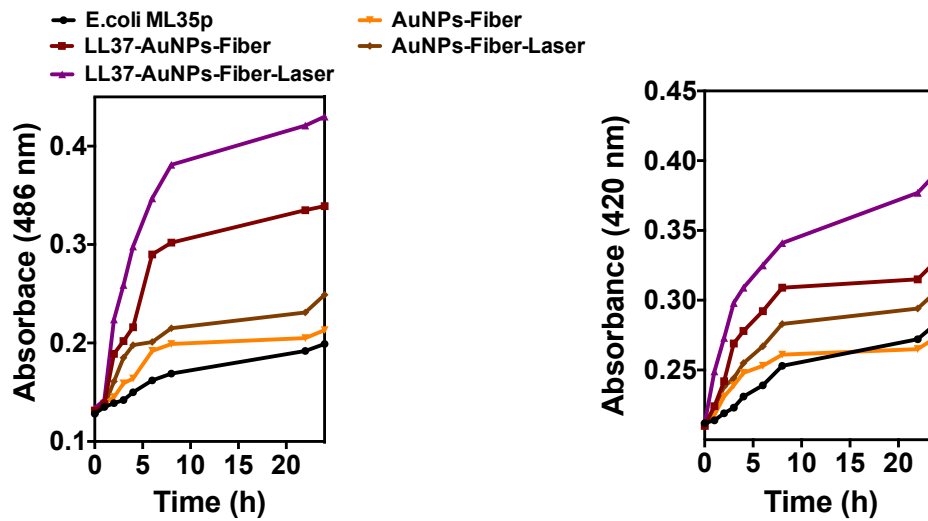


Figure 35-Permeabilization of the *E. coli* ML-35p membrane. On the left the results for the external membrane (OM) on the right those for the internal membrane (IM).

Testing with this engineered bacterium shows that both the outer and inner membranes are permeable. The only treatment that has no effect on the inner membrane is AuNPs-Fiber, as expected. The complete treatment, LL37-AuNPs exposed to the laser, is the best both in permeabilizing the external and internal membrane. We can observe a strong increase in the permeabilization of the external membrane already in the first hours. it is evident that much of the permeabilization is attributable to the formulation. The fibers with AuNPs, even if exposed to the laser, have a much milder effect.

## Conclusions

In this work a multifunctional platform for endodontic treatment has been proposed,. In each application, the risk of bacterial infections must be considered, even more so if the site is particularly exposed as in the case of dental applications. Endodontic interventions are carried out when dental and periodontal diseases, generally caused by normal oral microbiota infections, become severe. Such diseases cause pain, tooth erosion and loss. Dental restoration is a very common procedure but if the tooth is not cleaned well there is a high risk of developing bacteraemia (a secondary systemic infection dangerous especially for immunocompromised patients). Therefore, very powerful agents are used against bacteria (e.g. NaOCl) but they are also toxic which compromises the biological activity of stem cells of the root canal. Several efforts are being made to find viable alternatives to common antibiotics in order to limit bacterial resistance and, in a wider context, to preserve the self-healing abilities of the tissues. In this regard, the use of antimicrobial peptides (AMPs), such as LL37, in scientific research is increasingly widespread. LL37 is a complex peptide of which more and more functions are being discovered. In fact, it has immunomodulatory, chemotactic, angiogenesis properties and also differentiation properties that have recently been discovered.

The topical or systemic use of endogenous AMPs is limited by stability in the body environment due to the presence of proteases. The nanotechnology can overcome these challenges. Various alternative approaches have been proposed in the literature. Usually these are drug delivery systems, few examples of formulations with AMPs immobilized on surfaces or NPs. Some research has shown that this approach increases the bactericidal capacity (due to an increase in the local density of positive charges and peptide mass), the stability of AMPs and reduction in their enzymatic degradation. LL37-AuNP has a gold core and cysteine-modified LL37 coating [24]. Thanks to the one-step synthesis [46] process, the coating peptide itself is used as a capping agent for the reaction. In this way it is possible, at the same time, to control the physic-chemical properties of the NPs (e.g. size, charge...). Other NPs have been proposed for their antimicrobial effect (e.g. AgNPs) or for their ability to mineralize the matrix (NACP). Finding both features contained in one NP is not easy.

In this work we try to find other capacities of the LL37-AuNPs nanoformulation which has already proven to be very versatile (antimicrobial activity and wound healing) [24]. In particular, it has been shown that by exploiting the interaction between green laser and the core material of the LL37-AuNPs, the bactericidal effect increases. Thanks to an important optical property of AuNPs,

localized surface plasmon resonance (LSPR), the thermal energy generated by the laser light exposure of AuNPs helps to damage bacterial membranes. Theoretically, prolonged and high-power exposure kills more bacteria but the parameters for this experiment were chosen in a safe region for in vivo applications. Further studies are needed, such as general and point temperature monitoring to better understand how the green laser affects the antimicrobial test and whether it can be compatible with cell viability. The strategy of laser usage (three exposures of 1min spaced by 10sec of interruption) was effective but other combinations could be applied. The results against *S. aureus* are excellent, killing around 90% after 24 hours; against *S. epidermidis* and *E. coli* are maintained around 80% while *E. faecalis* only 70%. The *E. faecalis* is very common in dental and root canal infections. So, there is a need to optimize the parameters to fight the most resistant strains. A screening of various exposure times and interruptions could lead to the optimization of the treatment.

Furthermore, as far as we know, it is the first time that the differentiation potential of LL37 peptide has been studied on the stem cells from the apical papilla (SCAPs). In fact, another aim of the work is to regenerate the dental pulp by stimulating the differentiation of SCAPs into odontoblast cells [11]. From the results we learned that not only the free peptide induces differentiation but that nanoformulation LL37-AuNPs potentiates its effect. The results of the three different types of administration showed that LL37-AuNPs at low concentration (30µg/mL) prolonged the proliferation rate as well as the expression of EGFR of the SCAPs.

We found that AuNPs especially the colour of NP solution interferes in ALP and mineralization test. However, there are other ways to test the differentiation in the odontogenic sense of the cells that could solve these problems. For example, with RT-PCR and Western blot analysis it is possible to quantify the expression of specific genes and proteins of the various dental tissues (e. g. DSPP, BSP and OCN [11]) [42]. Furthermore, an efficient method for the quantification of Alizarin Red Staining which is necessary to confirm the results has not been found.

A major limitation in the analysis carried out is the number of donors. The current work was done with SCAP isolated from 1 patient's tooth. The experiments should be done with SCAPS isolated from several patient's teeth in order to validate the differentiation potential of LL37-AuNPs. The presence of bacterial infection can also alter the results [10]; therefore, the results should also be confirmed on infected models.

Finally, with a view to creating a tissue regeneration strategy, it was proposed to incorporate LL37-AuNPs on a support that mimics the extracellular matrix. It was chosen to make a nanofibres electrospun with a natural material, the gelatin. To ensure stability, a cross-linking method [59] was used which does not require post-processing of the fibers. Gelatin nanofibers conjugated with LL37-AuNPs were successfully tested against several bacterial strains. Although gelatin is not known for its antimicrobial properties, the results show a high bactericidal action. This is probably due to the high density of NPs present. Again, laser treatment has proven to be the most effective.

In future several experiments are needed to validate potential of LL37-AuNPs in dental application:

- Mechanical tests on gelatin fibers, after conjugation they could change and deteriorate.
- Quantification test of conjugated NPs on 2cm<sup>2</sup> of fibrous matrix. We have kept area of fiber constant throughout the experiment but the quantification of conjugated LL37-AuNPs on fibers is required to compare with LL37-AuNPs in solution.
- Adhesion assay to understand if conjugation of NPs affects cell adhesion [59].
- Cell viability, apoptosis assay or proliferation test to understand if the adhered cells are alive and healthy [59].
- Differentiation test. Rather than using traditional ALP and mineralization assays, western blot and rt-PCR analyses should be done to understand the biomarker present in odontoblast like cells.
- Furthermore, by exploiting the mechanical properties that the fiber offers, the combined response of stretched fibers with conjugated LL37-AuNPs could be tested.

In conclusion, the LL37-AuNPs nanoformulation proved to be antimicrobial against different bacterial strains and capable of stimulating the differentiation of SCAPs into odontoblasts. The laser exposure increased the bactericidal effect by damaging the bacterial membrane. The use of a gelatin nanofibrous scaffold has not disturbed the antimicrobial properties of LL37-AuNPs and promises well for tissue regeneration applications. More tests are needed to better understand the mechanisms involved but the evidence brought to light in this thesis work opens up to future developments in the field of endodontics and beyond.

## References

- [1] "Tissue engineering-Wikipedia," [Online]. Available: [https://en.wikipedia.org/wiki/Tissue\\_engineering](https://en.wikipedia.org/wiki/Tissue_engineering). [Accessed January 2020].
- [2] M. Y. A. I. D. A. Y. H. H. S. N. K. T. R. K.-N. Y. U. N. K. T. N. F. Y. T. Sonoda S, "Exogenous nitric oxide stimulates the odontogenic differentiation of rat dental pulp stem cells," *Scientific Reports*, p. 8(1):3419, 2018.
- [3] "Infodentis.com," [Online]. Available: <https://www.infodentis.com/tooth-anatomy/tooth-structure.php>. [Accessed January 2020].
- [4] "Tooth decay-Wikipedia," [Online]. Available: [https://en.wikipedia.org/wiki/Tooth\\_decay](https://en.wikipedia.org/wiki/Tooth_decay). [Accessed January 2020].
- [5] "Periodontal disease-Wikipedia," [Online]. Available: [https://en.wikipedia.org/wiki/Periodontal\\_disease](https://en.wikipedia.org/wiki/Periodontal_disease). [Accessed January 2020].
- [6] "Dental plaque-Wikipedia," [Online]. Available: [https://en.wikipedia.org/wiki/Dental\\_plaque](https://en.wikipedia.org/wiki/Dental_plaque). [Accessed January 2020].
- [7] "Dental abscess-Wikipedia," [Online]. Available: [https://en.wikipedia.org/wiki/Dental\\_abscess](https://en.wikipedia.org/wiki/Dental_abscess). [Accessed January 2020].
- [8] "Dental restoration-Wikipedia," [Online]. Available: [https://en.wikipedia.org/wiki/Dental\\_restoration](https://en.wikipedia.org/wiki/Dental_restoration). [Accessed January 2020].
- [9] V.-R. M. C. J. Baldión PA, "Odontoblast-Like Cells Differentiated from Dental Pulp Stem Cells Retain Their Phenotype after Subcultivation.," *International Journal of Cell Biology*, p. 2018:6853189, 2018.
- [10] D. R. T. K. P. L. E. C. D. A. R. S. K. D. R. N. Vishwanat L, "Effect of Bacterial Biofilm on the Osteogenic Differentiation of Stem Cells of Apical Papilla.," *Journal of Endodontics*, pp. 43(6):916-922, 2017.
- [11] L. G. V. J. T. A. G. P. K. P. G. W. Bakopoulou A, "Comparative analysis of in vitro osteo/odontogenic differentiation potential of human dental pulp stem cells (DPSCs) and stem cells from the apical papilla (SCAP).," *Archives of oral biology*, pp. 56(7):709-21, 2011.
- [12] "Bacteria-Wikipedia," [Online]. Available: <https://en.wikipedia.org/wiki/Bacteria>. [Accessed January 2020].
- [13] C. O. J. H. S. Z. M. C. J. P. M. S. G. M. T.-N. T. B. T. Højby N1, «The clinical impact of bacterial biofilms.», *International Journal of Oral Science*, pp. 3(2):55-65, 2011.
- [14] L. D. M. G. Reinaldo Ramos, «LL37, a human antimicrobial peptide with immunomodulatory properties,» in *Science against microbial pathogens: communicating current research and technological advances*, A. Méndez-Vilas (Ed.), 2011.

- [15] "Antimicrobial peptides: natural templates for synthetic membrane-active compounds.-Scientific Figure on ResearchGate," [Online]. Available: [https://www.researchgate.net/figure/Sketch-of-different-models-describing-the-functional-mechanisms-of-linear-antimicrobial\\_fig1\\_222711399](https://www.researchgate.net/figure/Sketch-of-different-models-describing-the-functional-mechanisms-of-linear-antimicrobial_fig1_222711399). [Accessed January 2020].
- [16] P. J. v. N. J. M. N. M. S. v. A. L. S. P. W. P. von Wintersdorff CJ, «Dissemination of Antimicrobial Resistance in Microbial Ecosystems through Horizontal Gene Transfer,» *Front Microbiol.*, p. 10.3389, 2016.
- [17] C. N., «The role of healthcare personnel in the maintenance and spread of methicillin-resistant Staphylococcus aureus.,» *J Infect Public Health.*, p. 10.3389, 2016.
- [18] K. K. B. A. Frieri M., «Antibiotic resistance,» *J Infect Public Health.*, pp. 10(4):369-378, 2017.
- [19] G. G. R. M. B. K. A. B. Johansson J, «Conformation-dependent antibacterial activity of the naturally occurring human peptide LL-37.,» *The Journal of Biological Chemistry*, pp. 273(6):3718-24, 1998.
- [20] J. H. L. H. C. C. B. Lee SH, "Antibacterial and lipopolysaccharide (LPS)-neutralising activity of human cationic antimicrobial peptides against periodontopathogens," *International Journal of Antimicrobial Agents*, pp. 35(2):138-45, 2010.
- [21] M. K. L. R. Tanaka D, "Sensitivity of Actinobacillus actinomycetemcomitans and Capnocytophaga spp. to the bactericidal action of LL-37: a cathelicidin found in human leukocytes and epithelium," *Oral Microbiology and Immunology*, pp. 15(4):226-31., 2000.
- [22] C. G. B. H. A. M. Pütsep K, «Deficiency of antibacterial peptides in patients with morbus Kostmann: an observation study,» *Lancet*, pp. 360(9340):1144-9, 2002.
- [23] S. U. R. A. Dürr UH, «LL-37, the only human member of the cathelicidin family of antimicrobial peptides.,» *Biochimica et Biophysica Acta* , pp. 1758(9):1408-25, 2006.
- [24] A. R. K. K. C. S. P. S. A. A. F. F. A. Z. J. B. R. C. R. R. J. L. P. N. S. V. P. L. F. Michela Comune, "Antimicrobial peptide-gold nanoscale therapeutic formulation with high skin regenerative potential," *Elsevier*, p. 10.1016, 2017.
- [25] v. H. M. Duplantier AJ, «The Human Cathelicidin Antimicrobial Peptide LL-37 as a Potential Treatment for Polymicrobial Infected Wounds,» *Frontiers in Immunology*, p. 4:143, 2013.
- [26] N. K. W. U. W. M. W. T. G. K. G. S. L. I. B. R. Piktel E, «The Role of Cathelicidin LL-37 in Cancer Development.,» *Archivum Immunologiae et Therapiae Experimentalis* , pp. 64(1):33-46, 2016.
- [27] Y. X. L. M. F. G. Z. Y. Y. S. I. C. Y. S. Liu Z, «Antimicrobial Peptide Combined with BMP2-Modified Mesenchymal Stem Cells Promotes Calvarial Repair in an Osteolytic Model.,» *Molecular Therapy*, pp. 26(1):199-207, 2018.
- [28] J. P. H. Y. L. H. S. L. Fu L, «The antimicrobial peptide KR-12 promotes the osteogenic differentiation of human bone marrow stem cells by stimulating BMP/SMAD signaling,» *Molecular Medicine Reports*, p. 10.3892, 2019.



- [29] d. B. P. d. L. Z. E. d. O. F. C. C. S. Milhan NVM, «The Antimicrobial Peptide LL-37 as a Possible Adjunct for the Proliferation and Differentiation of Dental Pulp Stem Cells,» *Journal of Endodontics*, pp. 43(12):2048-2053, 2017.
- [30] “Nanoparticle-Wikipedia,” [Online]. Available: <https://en.wikipedia.org/wiki/Nanoparticle>. [Accessed January 2020].
- [31] V. K. D. V. S. S. Tiwari PM, «Functionalized Gold Nanoparticles and Their Biomedical Applications.,» *Nanomaterials (Basel)*, pp. 1(1):31-63, 2011.
- [32] P. H., «Antimicrobial polymers with metal nanoparticles.,» *International Journal of Molecular Sciences*, pp. 16(1):2099-116, 2015.
- [33] F. A. D. S. L. F. Samiei M, «Nanoparticles for antimicrobial purposes in Endodontics: A systematic review of in vitro studies.,» *Materials Science & Engineering C-Materials for Biological Applications*, pp. 58:1269-78, 2016.
- [34] C. T. J. C. B. P. C. H. P. M. G. B. K. P. Bapat RA, «An overview of application of silver nanoparticles for biomaterials in dentistry.,» *Materials Science & Engineering C-Materials for Biological Applications*, pp. 91:881-898, 2018.
- [35] Y. R. T. A. C. A. V. P. G. P. S. V. Kushwaha V, «Comparative evaluation of antibacterial effect of nanoparticles and lasers against Endodontic Microbiota: An in vitro study.,» *Journal of Clinical and Experimental Dentistry*, pp. 10(12):e1155-e1160, 2018.
- [36] W. M. M. M. X. H. Wu J, «Development of novel self-healing and antibacterial dental composite containing calcium phosphate nanoparticles.,» *Journal of Dentistry*, n. 43(3):317-26, 2015.
- [37] E. A. A. E. F. A. S. K. M. A. A. Daraee H, «Application of gold nanoparticles in biomedical and drug delivery.,» *Artificial Cells, Nanomedicine, and Biotechnology*, pp. 44(1):410-22, 2016.
- [38] Y. F. P. Y. W. J. S. M. C. H. Y. V. Huang Y, «Co-administration of protein drugs with gold nanoparticles to enable percutaneous delivery.,» *Biomaterials*, p. 10.1016, 2010.
- [39] C. H. C. H. L. J. C. J. Lee JH, «Application of Gold Nanoparticle to Plasmonic Biosensors,» *International Journal of Molecular Sciences*, n. 19(7), 2018.
- [40] L. J. Z. J. W. X. K. N. C. G. Li J, «Gold nanoparticle size and shape influence on osteogenesis of mesenchymal stem cells.,» *Nanoscale*, pp. 8(15):7992-8007, 2016.
- [41] P. S. M. V. G. A. R. V. M. I. Singh P, «Gold Nanoparticles in Diagnostics and Therapeutics for Human Cancer.,» *International Journal of Molecular Sciences*, p. 19(7). pii: E1979, 2018.
- [42] L. D. F. C. Z. J. Y. M. Yi C, «Gold nanoparticles promote osteogenic differentiation of mesenchymal stem cells through p38 MAPK pathway.,» *ACS Nano*, pp. 4(11):6439-48, 2010.
- [43] Y. C. N. K. G. C. J Li, «Ligand density-dependent influence of arginine–glycine– aspartate functionalized gold nanoparticles on osteogenic and adipogenic differentiation of mesenchymal stem cells,» *Nano Research*, p. 1247–1261, 2018.

- [44] C. H. Z. F. B. C. W. M. R. M. M. J. G. N. X. H. Xia Y, «Gold nanoparticles in injectable calcium phosphate cement enhance osteogenic differentiation of human dental pulp stem cells,» *Nanomedicine: Nanotechnology, Biology and Medicine*, pp. 14(1):35-45, 2018.
- [45] P. S. E. M. G. H. K. S. F. M. F. L. Rai A, «High-density antimicrobial peptide coating with broad activity and low cytotoxicity against human cells.,» *Acta Biomaterialia*, p. Acta Biomaterialia, 2016.
- [46] P. S. V. T. F. A. M. C. T. U. E. M. C. M. R. K. S. P. M. L. F. L. Rai A, «One-step synthesis of high-density peptide-conjugated gold nanoparticles with antimicrobial efficacy in a systemic infection model,» *Biomaterials*, pp. 85:99-110, 2016.
- [47] R. A. P. S. E. M. C. R. P. C. C. T. P. A. I. M. S. A. D. L. P. A. F. L. Maleki H, «High Antimicrobial Activity and Low Human Cell Cytotoxicity of Core-Shell Magnetic Nanoparticles Functionalized with an Antimicrobial Peptide.,» *ACS Applied Materials & Interfaces*, pp. 8(18):11366-78, 2016.
- [48] R. A. C. K. P. S. A. S. F. A. Z. A. B. J. C. R. R. R. L. J. S. P. P. V. F. L. Comune M, «Antimicrobial peptide-gold nanoscale therapeutic formulation with high skin regenerative potential.,» *J Control Release*, p. 10.1016, 2017.
- [49] A. M. R. K. J. S. S Arcidiacono, «Kinetic microplate assay for determining immobilized antimicrobial peptide activity,» *Analytical biochemistry*, 2011.
- [50] «Changchun New Industries Optoelectronics Technology Co.-lasersciences.com,» [Online]. Available: [lasersciences.com/green-laser/57543110.html](http://lasersciences.com/green-laser/57543110.html). [Consultato il giorno December 2019].
- [51] «Diode-pumped solid-state laser, Wikipedia,» [Online]. Available: [https://en.wikipedia.org/wiki/Diode-pumped\\_solid-state\\_laser](https://en.wikipedia.org/wiki/Diode-pumped_solid-state_laser). [Consultato il giorno December 2019].
- [52] C. M. Otvos L., «Broth microdilution antibacterial assay of peptides,» *Methods Mol Biol.*, p. 10.1007, 2007.
- [53] P. J. W. J. S. P. E. R. Epand RF, «Depolarization, Bacterial Membrane Composition, and the Antimicrobial Action of Ceragenins,» *Antimicrob Agents Chemother*, pp. 54(9):3708-13, 2010 .
- [54] M. KM, «Flow Cytometry: An Overview.,» *Current Protocols in Immunology*, pp. 120:5.1.1-5.1.11, 2018.
- [55] V. M. N. M. N. J. B. M. Albuquerque MT, «Tissue-engineering-based strategies for regenerative endodontics.,» *Journal of Dental Research*, pp. 93(12):1222-31, 2014.
- [56] P. D. N. J. Bottino MC, «Advanced Scaffolds for Dental Pulp and Periodontal Regeneration.,» *Dental Clinics of North America*, pp. 61(4):689-711, 2017.
- [57] K. B. W. A. C. S. W. H. M. J. J. H. C. K. Kaushik SN, «Biomimetic microenvironments for regenerative endodontics.,» *Biomaterials Research*, p. 20:14, 2016.

- [58] M. G. G. D. Rodríguez-Tobías H, «Comprehensive review on electrospinning techniques as versatile approaches toward antimicrobial biopolymeric composite fibers.,» *Materials Science & Engineering C-Materials for Biological Applications*, pp. 101:306-322, 2019.
- [59] C. E. G. S. C. V. M. C. G. P. P. I. Z. M. C. G. Tonda-Turo C, «Crosslinked gelatin nanofibres: preparation, characterisation and in vitro studies using glial-like cells.,» *Mater Sci Eng C Mater Biol Appl.*, p. 10.1016, 2013.
- [60] C. N. N. F. S. D. L. Campiglio CE, «Cross-Linking Strategies for Electrospun Gelatin Scaffolds.,» *Materials (Basel, Switzerland)*, p. 12(15). pii: E2476., 2019.
- [61] R. F. C. C. G. P. V. P. F. A. F. L. C. G. Tonda-Turo C, «Nanostructured scaffold with biomimetic and antibacterial properties for wound healing produced by 'green electrospinning'.»,» *Colloids and Surfaces B: Biointerfaces* , pp. 172:233-243, 2018.
- [62] T.-T. C. D. P. D. R. F. G. G. N. S. C. V. G. M. M. V. C. G. C. G. Marino A, «Gelatin/nanoceria nanocomposite fibers as antioxidant scaffolds for neuronal regeneration.,» *Biochimica et Biophysica Acta - General Subjects* , pp. 1861(2):386-395, 2017.
- [63] S. H. A. M. G. A. Y. T. Abdelhamid S, «Laser-induced modifications of gold nanoparticles and their cytotoxic effect.,» *Journal of Biomedical Optics*, p. 17(6):068001, 2012.
- [64] D. W. T. U. S Hashimoto, «Studies on the interaction of pulsed lasers with plasmonic gold nanoparticles,» *Journal of Photochemistry and Photobiology* , p. 26, 2012.
- [65] O. K. I. H. I. E. Kuroda K, «The Human Cathelicidin Antimicrobial Peptide LL-37 and Mimics are Potential Anticancer Drugs.,» *Frontiers in Oncology*, p. 5:144, 2015.
- [66] «Celltiter-Glo Luminescent Cell Viability Assay protocol,» [Online]. Available: <https://ita.promega.com/resources/protocols/technical-bulletins/0/celltiter-glo-luminescent-cell-viability-assay-protocol/>.
- [67] «Flow cytometry-Wikipedia,» [Online]. Available: [https://en.wikipedia.org/wiki/Flow\\_cytometry](https://en.wikipedia.org/wiki/Flow_cytometry). [Consultato il giorno February 2020].
- [68] «Benchtop flow cytometer by BD Biosciences-BioOptics world,» [Online]. Available: <https://www.bioopticsworld.com/bioimaging/fluorescence/article/16432497/benchtop-flow-cytometer-by-bd-biosciences>. [Consultato il giorno February 2020].